Global Biogeochemical Cycles

RESEARCH ARTICLE
10.1029/2020GB006719

Key Points:
- Dissolved organic matter (DOM) from diverse circumpolar regions showed compositional and optical commonalities
- Added acetate and nutrients suppressed background DOM degradation but accelerated colored DOM breakdown
- Disconnect between DOM composition and function indicates intrinsic and extrinsic conditions interact to regulate DOM dynamics

Supporting Information:
- Supporting Information S1
- Data Set S1

Correspondence to:
S. A. Ewing and B. W. Abbott,
stephanie.ewing@montana.edu;
benabbott@byu.edu

Citation:
Wologo, E., Shakil, S., Zolkos, S., Textor, S., Ewing, S., Klassen, J., et al. (2021). Stream dissolved organic matter in permafrost regions shows surprising compositional similarities but negative priming and nutrient effects. *Global Biogeochemical Cycles*, *35*, e2020GB006719. https://doi.org/10.1029/2020GB006719

Received 25 JUN 2020
Accepted 22 SEP 2020
Accepted article online 18 NOV 2020

Stream Dissolved Organic Matter in Permafrost Regions Shows Surprising Compositional Similarities but Negative Priming and Nutrient Effects

Ethan Wologo[1], Sarah Shakil[2], Scott Zolkos[2,3], Sadie Textor[4], Stephanie Ewing[1], Jane Klassen[1], Robert G. M. Spencer[4], David C. Podgorski[4], Suzanne E. Tank[2], Michelle A. Baker[5], Jonathan A. O'Donnell[6], Kimberly P. Wickland[7], Sydney S. W. Foks[7], Jay P. Zarnetske[8], Joseph Lee-Cullin[8], Futing Liu[9], Yuanhe Yang[9], Pirkko Kortelainen[10], Jaana Kolehmainen[10], Joshua F. Dean[11,12], Jorien E. Vonk[11], Robert M. Holmes[3], Gilles Pinay[13], Michaela M. Powell[1], Jansen Howe[14], Rebecca J. Frei[14,15], Samuel P. Bratsman[14], and Benjamin W. Abbott[14]

[1]Department of Land Resources and Environmental Sciences, Montana State University, Bozeman, MT, USA, [2]Department of Biological Sciences, University of Alberta, Edmonton, Alberta, Canada, [3]Woods Hole Research Center, Woods Hole, MA, USA, [4]Department of Earth, Ocean and Atmospheric Science and National High Magnetic Field Laboratory Geochemistry Group, Florida State University, Tallahassee, FL, USA, [5]Department of Biology and Ecology Center, Utah State University, Logan, UT, USA, [6]Arctic Network, National Parks Service, Anchorage, AK, USA, [7]Water Resources Mission Area, USGS, Boulder, CO, USA, [8]Department of Earth and Environmental Sciences, Michigan State University, East Lansing, MI, USA, [9]State Key Laboratory of Vegetation and Environmental Change, Institute of Botany, Chinese Academy of Sciences, Beijing, China, [10]Finnish Environment Institute SYKE, Joensuu, Finland, [11]Department of Earth Sciences, Vrije Universiteit Amsterdam, Amsterdam, Netherlands, [12]School of Environmental Sciences, University of Liverpool, Liverpool, UK, [13]Environnement-Ville-Société (UMR5600) - Centre National de la Recherche Scientifique (CNRS), Lyon, France, [14]Department of Plant and Wildlife Sciences, Brigham Young University, Provo, UT, USA, [15]Department of Renewable Resources, University of Alberta, Edmonton, Alberta, Canada

Abstract Permafrost degradation is delivering bioavailable dissolved organic matter (DOM) and inorganic nutrients to surface water networks. While these permafrost subsidies represent a small portion of total fluvial DOM and nutrient fluxes, they could influence food webs and net ecosystem carbon balance via priming or nutrient effects that destabilize background DOM. We investigated how addition of biolabile carbon (acetate) and inorganic nutrients (nitrogen and phosphorus) affected DOM decomposition with 28-day incubations. We incubated late-summer stream water from 23 locations nested in seven northern or high-altitude regions in Asia, Europe, and North America. DOM loss ranged from 3% to 52%, showing a variety of longitudinal patterns within stream networks. DOM optical properties varied widely, but DOM showed compositional similarity based on Fourier transform ion cyclotron resonance mass spectrometry (FT-ICR MS) analysis. Addition of acetate and nutrients decreased bulk DOM mineralization (i.e., negative priming), with more negative effects on biodegradable DOM but neutral or positive effects on stable DOM. Unexpectedly, acetate and nutrients triggered breakdown of colored DOM (CDOM), with median decreases of 1.6% in the control and 22% in the amended treatment. Additionally, the uptake of added acetate was strongly limited by nutrient availability across sites. These findings suggest that biolabile DOM and nutrients released from degrading permafrost may decrease background DOM mineralization but alter stoichiometry and light conditions in receiving waterbodies. We conclude that priming and nutrient effects are coupled in northern aquatic ecosystems and that quantifying two-way interactions between DOM properties and environmental conditions could resolve conflicting observations about the drivers of DOM in permafrost zone waterways.

1. Introduction

Climate change is degrading permafrost at continental scales (Biskaborn et al., 2019; Jorgenson et al., 2018; Nitze et al., 2018; Olefeldt et al., 2016). Though the specific consequences of permafrost degradation depend on local conditions (Frey & McClelland, 2009; Littlefair et al., 2017; Tank et al., 2012, 2020; Toohey et al., 2016; Zolkos & Tank, 2020), the thawing of frozen material and associated changes in water flow

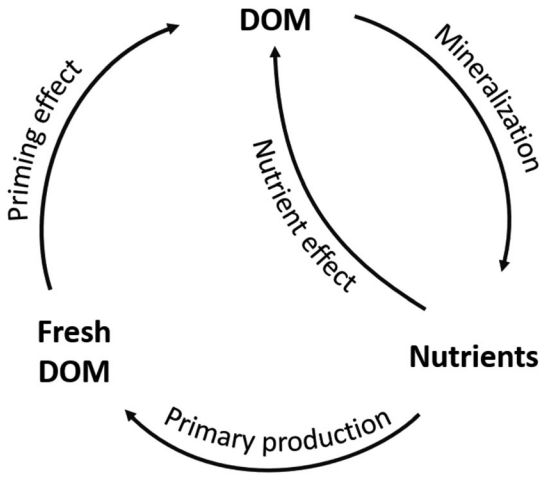

Figure 1. Schematic diagram of linkages between nutrient and priming effects in low-nutrient ecosystems. Arrows represent processes that produce or influence the various pools of dissolved organic matter (DOM) and nutrients. For example, nutrients stimulate primary production, which creates fresh DOM. Subsequently, fresh DOM may exert a positive or negative priming effect on the overall DOM pool. In eutrophic ecosystems such as agricultural and urban environments, nutrient effects can be decoupled from priming by the addition of anthropogenic nutrients and removal of fresh DOM sources during harvesting.

are causing release of dissolved organic matter (DOM) and inorganic nutrients such as nitrogen (N) and phosphorous (P) to streams, lakes, and coastal zones (Kendrick et al., 2018; O'Donnell, Aiken, Swanson, et al., 2016; Tanski et al., 2017; Treat et al., 2016; Vonk, Tank, Bowden, et al., 2015; Wickland et al., 2018). Though permafrost-derived DOM is often hundreds to tens of thousands of years old, it can be highly biolabile (Abbott et al., 2014; Drake et al., 2015; Ewing et al., 2015; Liu et al., 2019; Vonk et al., 2013) and photodegradable (Cory et al., 2013; Vonk, Tank, Bowden, et al., 2015), depending on source and permafrost type (Stubbins et al., 2016; Wickland et al., 2018). Consequently, some permafrost-derived DOM can be rapidly mineralized in headwater streams (Drake et al., 2015; Mann et al., 2015; Spencer et al., 2015; Vonk, Tank, Mann, et al., 2015; Wickland et al., 2012). Waterways in the permafrost zone already transport globally relevant amounts of DOM and nutrients (Holmes et al., 2012; McClelland et al., 2014). For example, Arctic and Boreal surface waters receive ~100 Tg of dissolved organic carbon (DOC) each year from terrestrial ecosystems, a third of which (~35 Tg C yr^{-1}) they deliver to the Arctic Ocean and surrounding seas (Abbott, Jones, et al., 2016; Kicklighter et al., 2013; McGuire et al., 2009). Radiocarbon measurements suggest that more than 80% of this DOC is modern—fixed since the 1950s (Qu et al., 2017; Raymond et al., 2007; Wild et al., 2019)—and even under extreme warming scenarios, DOM from degrading permafrost will likely remain a small proportion of total DOM flux (Abbott et al., 2015; Abbott, Jones, et al., 2016; Estop-Aragonés et al., 2020; Laudon et al., 2012). However, when biolabile DOC (BDOC) and nutrients from permafrost mix with modern DOM, they could influence mineralization rates and alter the net ecosystem carbon balance of the permafrost zone (Abbott et al., 2014; Larouche et al., 2015; Textor et al., 2019), potentially resulting in greater CO_2 efflux from permafrost ecosystems to the atmosphere.

Rates of DOM mineralization depend on the intrinsic properties of the DOM such as chemical composition as well as external conditions such as temperature, microbial community structure, and interactions with other elements (Abbott, Baranov, et al., 2016; Arnosti, 2004; Frei et al., 2020; Marín-Spiotta et al., 2014; Nalven et al., 2020; Zarnetske et al., 2011). Even DOM that has low inherent reactivity because of its source or prior processing may undergo further mineralization and transformation when mixed with BDOC or inorganic nutrients (Bianchi, 2012; Guenet et al., 2010; Kuzyakov et al., 2000; Mutschlecner et al., 2018; Rosemond et al., 2015). The addition of BDOC and nutrients may relieve energy and stoichiometric limitations of decomposers, accelerating mineralization of stable organic matter in the short term and altering the type of organic matter exported in the long term (Chen et al., 2019; Guenet et al., 2010; Lynch et al., 2018; Mack et al., 2004; Mutschlecner et al., 2017; Rosemond et al., 2015) (Figure 1). These priming and nutrient effects were initially observed in terrestrial environments during the last century (Bingemann et al., 1953; Blagodatsky & Richter, 1998; Broadbent, 1947; Jenkinson et al., 1985; Löhnis, 1926), but until the last decade, they had been largely untested in aquatic environments (Bianchi, 2011; Guenet et al., 2010; Marín-Spiotta et al., 2014). Recent aquatic priming studies have produced conflicting results, detecting aquatic priming effects in some environments (Bianchi et al., 2015; Guenet et al., 2014) but not others (Bengtsson et al., 2015; Catalán et al., 2015; Textor et al., 2018, 2019). The prevalence of priming and nutrient effects in high-latitude aquatic ecosystems remains an important source of uncertainty in estimates of the magnitude and timing of the permafrost climate feedback (Abbott, Jones, et al., 2016; Holmes et al., 2008; Keuper et al., 2020; Tank et al., 2020; Textor et al., 2019; Wickland et al., 2012).

While priming and nutrient effects have been considered independently, even in the few studies where both were measured (Guenet et al., 2014; Hotchkiss et al., 2014; Jenkinson et al., 1985), they are likely functionally linked, at least in oligotrophic and mesotrophic ecosystems (Figure 1). In the absence of external nutrient inputs from humans or other sources (Brahney et al., 2014; Frei et al., 2020), DOM mineralization is the proximate source of nutrients in terrestrial and aquatic ecosystems (Fork et al., 2020; McDowell et al., 2006; Mutschlecner et al., 2017), meaning that increased DOM biodegradability may increase nutrient availability.

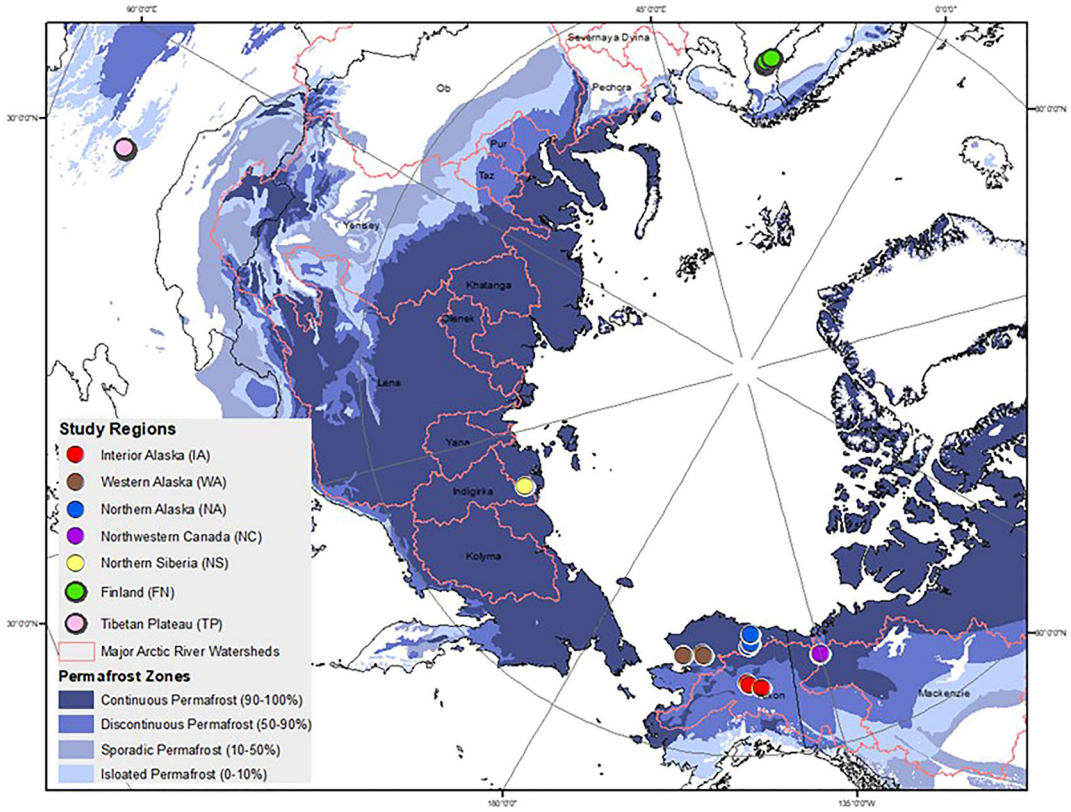

Figure 2. Map of sampling locations (colored circles), major Arctic watersheds, and permafrost distribution (Brown et al., 2002). See Table 1 for site details.

In turn, nutrient-rich environments support higher rates of primary productivity, root exudation, and production of more decomposable organic matter (Carey et al., 2019; Guenet et al., 2010; Hewitt et al., 2018; Mutschlecner et al., 2017; Salmon et al., 2018), increasing BDOC availability (Figure 1). The linkage between priming and nutrient effects complicates the interpretation of observational and experimental studies that only quantify one of the effects, because responses attributed to nutrients could be due to priming, and vice versa (Chen et al., 2019; Danger et al., 2013; Rosemond et al., 2015). Additionally, strong seasonal variation in nutrient concentrations and DOM properties can complicate comparison across studies (Holmes et al., 2008; Kortelainen et al., 2020; Wickland et al., 2012).

Here, we report results from an international experiment where we investigated the prevalence of priming and nutrient effects in 23 permafrost-zone streams from seven high-latitude or high-altitude regions. We sampled streams in the late summer in Alaska, Canada, Siberia, Finland, and the Tibetan Plateau (Figure 2 and Table 1). Our primary objectives were to (1) identify large-scale patterns of DOM molecular composition and metabolic stability in stream ecosystems across the permafrost zone, (2) quantify how additions of BDOC and nutrients affect modern DOM mineralization in diverse permafrost-zone ecosystems, and (3) test how stream network position affects DOM dynamics. Based on findings from terrestrial and aquatic priming studies in other regions (Chen et al., 2019; Dorado-García et al., 2015; Guenet et al., 2014), we hypothesized that the effects of BDOC and nutrient addition (i.e., the magnitude of priming and nutrient effects) would depend on background DOM composition and availability of nutrients. Following observations and hypotheses about DOM dynamics in high-latitude stream networks (Cory et al., 2014; Drake et al., 2015; Vonk, Tank, Mann, et al., 2015; Zarnetske et al., 2018), we hypothesized that DOC biolability would decrease longitudinally (i.e., larger rivers would have lower BDOC) because of longer transport times in soils and in-stream photodegradation and biodegradation (Catalán et al., 2016; Connolly et al., 2018; Creed et al., 2015; Shogren et al., 2019). We predicted larger priming and nutrient effects at sites with more stable DOC and lower nutrient availability, respectively. To test these predictions, we measured DOC

Table 1
Site Characteristics

Region	Site code[a]	Latitude (DD)	Longitude (DD)	Permafrost zone	Dominant vegetation type	Geologic substrate and texture	Watershed contributing area (km^2)	MAT (°C)/MAP (mm)	Major River Network
Interior Alaska	IA1	65.8007	−149.4392	Discontinuous	Black Spruce, moss, lichen, and low shrub	Loess (fine)	14	−7.5/270 (Ewing et al., 2015; Koch et al., 2014)	Yukon
	IA2	65.6540	−149.0921				12		
	IA3	65.3440	−146.9110			Loess, colluvium (mixed)	4		
Western Alaska	WA1	67.4830	−162.2150	Continuous	Sedge, dwarf shrub, and moss tundra	Glacial alluvium (coarse)	37	−5/300–400 (O'Donnell, Aiken, Butler, et al., 2016)	Noatak
	WA2	67.4740	−162.2250				748		
	WA3	67.7510	−158.1150	Continuous	Sedge, low shrub, and moss wetland	Glaciolacustrine (stratified-mixed)	1,165		
	WA4	67.8450	−158.3160				2,860		
Northern Alaska	NA1	68.6867	−149.0975	Continuous	Tussock-sedge, dwarf shrub, and moss tundra	Glacial till, loess (fine)	76	−10/320 (Abbott et al., 2015)	Sagavanirktok
	NA2	68.8772	−148.8445				3,604		
	NA3	69.6299	−148.6514				9,369		
Northwestern Canada	NC1	67.2517	−135.2716	Continuous	Black Spruce	Glacial till (fine)	5	−7.3/146 (Littlefair et al., 2017)	Peel
	NC2	67.3133	−135.1683				40		
	NC3	67.3360	−134.8714				71,658		
Northeastern Siberian	NS1	70.8317	147.5173	Continuous	Tussock-sedge, dwarf and low shrub, and moss tundra	Silt (fine)	<1	−10.5/212 (Iwahana et al., 2014)	Indigirka
	NS2	70.8300	147.5118				122		
	NS3	70.8226	147.5135				14,600		
Finland	FN1	66.1478	26.1618	Non-permafrost	Boreal forest/ peatland/ agriculture	Glacial till and peatlands (fine)	62	1.7-2.8/560-644 (de Wit et al., 2020; Lepistö et al., 2008; Mattsson et al., 2005)	Simojoki
	FN2	65.9529	25.9342				1,919		
	FN3	65.6618	25.0754				3,093		
Tibetan Plateau	TP1	37.4776	100.2885	Discontinuous	Swamp Meadow	Silt-loam (fine)	4	−3.3/460 (Liu et al., 2018)	Shaliu
	TP2	37.4182	100.2392				32		
	TP3	37.3468	100.2259				420		

[a]The sites in each region were nested within the same watershed, except Interior Alaska.

disappearance in 28-day incubations with and without acetate and inorganic nutrient additions. We quantified priming and nutrient effects by measuring acetate and background DOC drawdown and by characterizing background DOM composition by fluorescence spectroscopy and Fourier transform ion cyclotron resonance mass spectrometry (FT-ICR MS).

2. Methods

We collected stream samples from August to September 2016 from six regions across the permafrost zone and in September 2017 from one northern, non-permafrost region (Figure 2). Water samples were collected from three or more locations within each study region. Regions were selected to include Arctic, boreal, and alpine ecosystem types and to represent a range of current and future climatic conditions in the permafrost zone (continuous, discontinuous, and non-permafrost; Table 1). Samples were collected during late summer when background DOC biolability is typically lowest (Holmes et al., 2008; Mu et al., 2017; Wickland et al., 2012) and when permafrost DOC and nutrients are most likely to influence aquatic ecosystems during the period of maximum annual thaw (Abbott et al., 2014, 2015; Treat et al., 2016). To test our hypothesis about longitudinal (upstream-downstream) patterns in DOM composition (Cory et al., 2014; Drake et al., 2015; Shogren et al., 2019), we selected sites that were nested in river networks, except in interior Alaska, where the three sites came from independent streams because of accessibility considerations. Our naming convention was a two-letter acronym of the region name and a number starting from the smallest catchment (Table 1). In western Alaska, where we had two sets of nested catchments, WA1 was upstream of WA2 in one network, and WA3 was upstream of WA4 in a second network.

2.1. Characterization of Study Regions

For each region, we characterized a suite of ecological characteristics. We first delineated contributing watershed areas in ArcGIS (most sites) or Google Earth (Tibetan Plateau sites). For each watershed, we

determined physical and textural properties of lithologic substrate using maps of surficial geology and descriptions from the literature (Hamilton, 2003; Kokelj et al., 2017; Yang et al., 2010). We classified each watershed as continuous permafrost (>90% of land surface underlain by permafrost), discontinuous permafrost (50–90%), or permafrost free (Brown et al., 1997). Lastly, we identified dominant vegetation types with the Circumpolar Arctic Vegetation Map (Walker et al., 2018) or referenced literature (Table 1).

The seven sampled regions include broad variation in climate, geology, topography, and vegetation (Table 1). Mean annual temperature (MAT) ranges from −5°C to −10.5°C across the permafrost-affected sites and is 1.7°C to 2.8°C at the non-permafrost sites in Finland. Mean annual precipitation (MAP) ranges from 140 to 600 mm (Table 1). In all permafrost-affected regions, various types of permafrost degradation have been observed, including thermokarst and thermo-erosional features such as retrogressive thaw slumps, thermo-erosional gullies, and thermokarst lakes (Aanderud et al., 2019; Farquharson et al., 2019; Littlefair & Tank, 2018; Liu et al., 2019; Luo et al., 2019; Mu et al., 2019; Olefeldt et al., 2016). Other forms of less visible permafrost warming and degradation are also occurring in the study areas, including active-layer thickening and talik (pockets of permanently thawed material) formation (Biskaborn et al., 2019; Shiklomanov et al., 2010; Vonk, Tank, Bowden, et al., 2015). Permafrost degradation across all the regions is projected to accelerate in the coming decades (Guo et al., 2012; Jafarov et al., 2018; Nicolsky et al., 2017; Romanovsky et al., 2010; Turetsky et al., 2020; Wang et al., 2020).

Though permafrost degradation is present in all the studied permafrost catchments, three of the seven regions (Canada, interior Alaska, and the Tibetan Plateau) were specifically chosen for their proximity to abrupt thaw features. The northwestern Canada Sites NC1 and NC2, which are underlain by glacial tills, drain watershed areas downstream of a large thaw slump—Site "FM3" in other studies (e.g., Littlefair et al., 2017). Site NC3 is located on the mainstem of the larger Peel River, which receives inputs from numerous slump-affected tributaries (Kokelj et al., 2017; Littlefair & Tank, 2018; Zolkos et al., 2018). The interior Alaska Sites IA1 and IA2, which occur in thick, ice-rich Pleistocene silt (Yedoma), are adjacent to a thawing pingo and thermokarst channel, respectively (Ewing et al., 2015; Koch et al., 2013). Site IA3 is a gravel bedded stream draining a partially burned watershed with limited loess cover and some isolated thermokarst features (Koch et al., 2014). The Tibetan Plateau sites are downstream of a thermo-erosional gully in a silt-dominated alpine swamp meadow (Chen et al., 2018; Liu et al., 2018). Even for these thaw-adjacent sites, the current contribution of permafrost DOM and nutrients in the sampled streams is likely small because of dilution (Abbott et al., 2015; Larouche et al., 2015). However, we included sites in areas of actively degrading permafrost because thermokarst-prone areas contain approximately half of permafrost-zone organic matter and may contribute more than half of the permafrost climate feedback (Olefeldt et al., 2016; Turetsky et al., 2020).

The Siberian Site NS1 is a small pond that is connected to the river network via surface flow during high flows, while Sites NS2 and NS3 are part of the mainstem downstream of NS1 (Dean et al., 2020). The watersheds in western Alaska are underlain by continuous permafrost but differ with respect to topography and permafrost soil properties. Sites WA1 and WA2 drain an alpine watershed underlain by ice-poor permafrost and parent material composed of glacially derived gravel and cobble substrate (O'Donnell, Aiken, Butler, et al., 2016). WA3 and WA4 drain an ice-rich watershed with numerous thermokarst lakes and slumps in the catchment, though not adjacent to the sampling sites (O'Donnell, Aiken, Butler, et al., 2016). The northern Alaska sites occur in Arctic tundra and are underlain by continuous permafrost. NA1 is a stream called Oksrukuyik Creek that drains moist tundra with numerous thermokarst lakes in the catchment (Shogren et al., 2019). NA2 and NA3 are on the mainstem Sagavanirktok River, which is fed mostly by glacial runoff from the Brooks Range (Abbott et al., 2014; Cory et al., 2014; Hamilton, 2003). The Finnish sites represent a non-permafrost region in the subarctic characterized by boreal forest and peatlands (Lepistö et al., 2008; Mattsson et al., 2005), providing an analog for future conditions in much of the permafrost zone.

2.2. Sample Collection and Incubation Setup

For the incubation, we followed the standardized protocol proposed by Vonk, Tank, Mann, et al. (2015), with minor modifications to suit the field conditions and laboratory analyses (SI: detailed protocol). Incubations were performed locally by each regional team, and samples were shipped to centralized locations for analysis (details in section 2.3). Stream water was filtered on site (0.7 μm, Whatman GF/F), and refrigerated until laboratory incubations were initiated. Incubations were started within 1 or 2 days after sample collection

except for the western Alaska (WA) and the northeastern Siberian (NS) sites, which were initiated one week after sample collection due to field constraints.

For incubations, we divided the filtered bulk stream samples into 200-ml aliquots and treated each aliquot with one of eight acetate (CH_3COO^-) and nutrient treatments (Table S1; Abbott & Ewing, 2020). We used acetate as the priming substrate in these experiments for three reasons: (1) Acetate is a highly biolabile form of DOC often used in ecosystem manipulations (Robbins et al., 2017; Zarnetske et al., 2011); (2) it is easily measurable via ion chromatography, allowing us to directly quantify disappearance of added substrate and background DOC (Baker et al., 1999; Hotchkiss et al., 2014); and (3) acetate naturally accumulates in permafrost during anaerobic metabolism and is released during permafrost thaw, representing up to a quarter of total permafrost DOC in some areas (Drake et al., 2015; Ewing et al., 2015; Neumann et al., 2016). We used ammonium (NH_4^+), nitrate (NO_3^-), and phosphate (PO_4^{3-}) as the inorganic nutrient substrates. These inorganic nutrients are commonly used in nutrient enrichment studies (Rosemond et al., 2015; Slavik et al., 2004), and they are released during permafrost degradation (Abbott et al., 2015; Keuper et al., 2017). We set treatment levels of acetate and nutrients (Table S1) based on observed concentrations of low-molecular weight DOC and inorganic nutrients in streams draining thermokarst features (Abbott et al., 2014, 2015; Drake et al., 2015; Ewing et al., 2015; Tanski et al., 2017). The three acetate-only treatment levels (A1, A2, and A3) had 1, 5, and 10 mg C L^{-1} of added acetate, respectively. The three nutrient-only treatment levels (N1, N2, and N3) had a 25:5:1 blend of different concentrations of NH_4^+, NO_3^-, and PO_4^{3-} (Table S1), based on observed ratios of these nutrients in thermokarst outflows (Abbott et al., 2015). The remaining two treatments were a high acetate plus high nutrient treatment (AN) and a control sample (CT) in which only deionized water was added. Though background DOC and nutrient conditions varied among the sites, we kept the treatments consistent for comparison and to simulate how permafrost degradation may release concentrations of acetate and nutrients uncorrelated with modern in-stream conditions (Coch et al., 2020; Ewing et al., 2015; Tanski et al., 2017). While we recognize that micronutrients can limit microbial activity, we limited the experiment to carbon, nitrogen, and phosphorus additions for logistical reasons—for example, there is great diversity of observed micronutrients in permafrost waterways and soils (Carey et al., 2019; Krickov et al., 2020; Reyes & Lougheed, 2015).

We incubated water from each site in 24 borosilicate 250-ml brown glass bottles (three replicates of the eight treatments), which were generally kept stationary on a benchtop at each incubation location. Incubations were done in the dark at room temperature (20°C), constraining DOC loss to biotic rather than photic processes. The relatively coarse filtration (0.7-μm effective pore size) prior to incubation allowed ambient aquatic microorganisms to pass through the filter into the incubation bottles and mineralize the DOC (Dean et al., 2018; Larouche et al., 2015; Vonk, Tank, Mann, et al., 2015). Treatments were added only at the start of the incubations to simulate mixing of permafrost thaw products with modern DOM in stream networks (Abbott et al., 2015; Drake et al., 2015; Shogren et al., 2019; Tanski et al., 2017).

The incubation samples from the Tibetan Plateau sites were destroyed during shipping, but the background chemistry, optical samples, and molecular samples survived.

2.3. Background Chemistry, DOC, and Acetate Analyses

Incubation and baseline chemistry samples were collected, frozen, and sent for analysis at the Environmental Analytical Laboratory in the Department of Land Resources and Environmental Sciences at Montana State University (MSU). Inorganic nutrients (NH_4^+, NO_3^-, NO_2^-, and PO_4^{3-}) in unamended (background) stream waters were determined at μg L^{-1} levels on a QuAAtro39 continuous segmented flow analyzer (Seal Analytical, Inc.). We calculated dissolved inorganic nitrogen (DIN) as the sum of NH_4^+, NO_3^-, and NO_2^-. Acetate and other dissolved solutes in the treated incubation samples (NO_3^-, NO_2^-, and Cl^-) were measured at mg L^{-1} levels on an ICS 2100 Ion Chromatograph (Dionex, Thermo Scientific) equipped with an anion column (ASX-18 column). DOC and total nitrogen (TN) in all samples were determined using a V-TOC CSH Total Carbon Auto-Analyzer with a TNM-1 Total Nitrogen Module (Shimadzu Corporation). Analytical uncertainties were determined for each instrument based on replication of samples and results for several representative working standards (supporting information). Samples were kept frozen at MSU until analysis, and values were only accepted if uncertainty was less than 10%. When concentrations were below the limit of detection, we set their values to half the detection limit.

2.4. Optical Properties and Molecular Composition of DOM

We collected additional subsamples at t_0 and t_{28} from a subset of the treatments (CT, A3, and AN) for optical analysis via fluorescence spectroscopy. These subsamples were filter sterilized (0.22 μm, PES) into 40-ml amber glass vials and stored in the dark at 4°C during shipment and until analysis at Utah State University within four months of arrival (Baker & Lamont-BIack, 2001). We measured the absorbance and fluorescence of these subsamples with a spectrofluorometer (Aqualog, Horiba Scientific, Edison, New Jersey). We analyzed the absorbance data and the excitation emission matrices (EEMs) to calculate several common indices of DOM composition (Fellman, Spencer, et al., 2010; Kellerman et al., 2018; McKnight et al., 2001; Weishaar et al., 2003), including colored DOM (CDOM; absorbance at 254 nm), biological index (BIX), humification index (HIX), fluorescence index (FI), peak T (tryptophan-like) to peak C (fulvic/humic-like) index (TC), and specific ultraviolet (UV) absorbance at 254 nm ($SUVA_{254}$) (Gabor, Baker, et al., 2014; Gabor et al., 2015). Because the behavior of the ambient DOC was our primary focus, we subtracted the measured acetate concentration from total DOC concentration for the acetate-addition treatments before calculating $SUVA_{254}$ and other metrics (e.g., priming as described in section 2.5). All samples were corrected for inner filter effects, Rayleigh scatter, and blank subtraction in MATLAB™ (version 6.9; MathWorks, Natick, Massachusetts), and samples that exceeded 0.3 absorbance units at excitation 254 nm were diluted with deionized water to be under 0.3 absorbance units and re-run (reported values have been adjusted proportionally to the dilution factor).

We selected a subset of samples for analysis of DOM chemical composition via ultrahigh resolution mass spectrometry with a 21 T FT-ICR MS (Hendrickson et al., 2015; Smith et al., 2018). Because of the high cost of these analyses, we selected only the CT and A3 treatments at the t_0 and t_{28} time steps for a subset of sites (a total of 33 samples). These subsamples were filtered to 0.7 μm (GF/F pre-combusted at 450°C for 5 hr) to remove potential flocculation and stored frozen in pre-leached, high-density polyurethane bottles until analysis at the National High Magnetic Field Laboratory, Tallahassee, FL (Spencer et al., 2015; Textor et al., 2019). We used DOC concentration to calculate the appropriate volume for solid phase extraction (100-mg Bond Elut PPL, Agilent Technologies) following the method described by Dittmar et al. (2008) and aimed for a concentration of 40 μg C ml^{-1} for DOM extracts eluted with 1 ml of methanol. All FT-ICR MS samples were analyzed in negative ion mode and molecular formulae were examined in the mass range of 170–1,500 m/z and reassigned in PetroOrg Software (Corilo et al., 2013, 2016; Liu et al., 2016). We examined elemental combinations of $C_{1\text{-}45}$ $H_{1\text{-}92}N_{0\text{-}4}O_{1\text{-}25}S_{0\text{-}2}$ with mass errors less than 300 ppb and excluding noise signals >6σ root-mean-square (RMS) baseline (O'Donnell, Aiken, Butler, et al., 2016). Elemental stoichiometries and modified aromaticity indices (AI_{mod}) (Koch & Dittmar, 2016) were used to assign molecular formulae into seven different compound classes using a script developed by Hemingway (2018): *unsaturated phenolic low O/C* = $AI_{mod} < 0.5$, H/C < 1.5, O/C < 0.5; *unsaturated phenolic high O/C* = $AI_{mod} < 0.5$, H/C < 1.5, O/C ≥ 0.5; *polyphenolic* = AI_{mod} 0.50–0.67; *condensed aromatic* = $AI_{mod} > 0.67$; *aliphatic* = H/C ≥ 1.5, O/C < 0.9; *N* = 0; *sugar-like* = O/C > 0.9; and *peptide-like* = H/C ≥ 1.5, O/C < 0.9 *N* ≥ 1 (O'Donnell, Aiken, Swanson, et al., 2016). Although molecular peaks detected during FT-ICR-MS may represent multiple isomers, we interpret DOM composition based on the relative abundance of molecular formulae assigned to each compound class. Therefore, molecular formulae assigned to the same compound class may herein be collectively described as compounds.

2.5. Biodegradability, Priming, and Nutrient Effects

Hereafter, we refer to "background" DOC as the total DOC concentration minus added and ambient acetate. To calculate rates of acetate and background DOC consumption, we poured off and froze ~15 ml of sample into polypropylene vials immediately following the addition of treatments (t_0), after 7 days (t_7), and after 28 days (t_{28}). We calculated change in background DOC and acetate for each replicate individually as the proportional difference between the t_0 and t_7 or t_0 and t_{28} concentrations (e.g., a ΔDOC_7 of −0.2 represents a 20% decrease in DOC concentration or a BDOC value of 20% after 7 days). We then calculated the mean and standard deviation of ΔDOC and ΔAcetate across the three replicates for each site and time step. Replicates with evidence of contamination or analytical error were excluded from the means. We calculated change in optical properties (ΔOptical) and relative abundance (ΔRA) of molecular composition in the same way as ΔDOC and ΔAcetate.

We calculated priming and nutrient effects for each site as the ΔDOC in each treatment minus the ΔDOC in the unamended (control) treatment. This yielded positive values for the nutrient and priming effects when the treatment resulted in greater background DOC consumption (i.e., positive priming) and negative values when the treatment DOC consumption was less than the control (i.e., negative priming), following the typical sign convention (Bianchi et al., 2015; Guenet et al., 2010; Hotchkiss et al., 2014).

2.6. Statistical Analyses

To test for differences in ΔDOC, ΔAcetate, ΔOptical, and ΔRA among treatments, we used one-way analysis of variance (ANOVA) with site as a blocking factor to account for non-independence (Malone et al., 2018). We tested if priming effects were different across time steps for the various treatments with a two-way ANOVA, also with site as a blocking factor. For all ANOVAs, we used Tukey's honest significant difference post hoc tests for multiple comparisons with a Bonferroni correction and a decision criterion of $\alpha = 0.05$. We evaluated normality, homoscedasticity, and leverage (Cook's distance) for each test visually. To evaluate if nutrient and priming effects were significant (i.e., statistically different than 0), we used two-sided *t* tests for each treatment, interpreted after a Bonferroni correction.

To evaluate similarity of DOM compounds and optical properties across sites, we used principal component analysis (PCA). We scaled all parameters to have a mean of 0 and a variance of 1, and we transformed the non-normally distributed parameters to avoid undue influence from extreme observations and to allow the computation of parametric probability ellipses (Kotz & Nadarajah, 2004). We used the Kaiser criterion, scree plots, and the percent explained variance to decide how many principal components to report (Horikoshi et al., 2020; Wickham et al., 2020).

To test our hypotheses about links between priming and nutrient effects, we used Spearman rank correlations (ρ) to quantify relationships (including non-linear relationships) among BDOC, priming/nutrient effects, and background nutrient chemistry. We evaluated relationships with background DOC, DIN, PO_4^{3-}, and the molar ratios of those parameters (DOC:DIN, DOC:PO_4^{3-}, and DIN:PO_4^{3-}), using a decision criterion of $\alpha = 0.05$. Finally, we used Spearman rank correlations to test for links between water chemistry, climate variables (i.e., MAT and MAP), and watershed area.

All statistical analyses were performed in R.3.5.0 (R Core Team, 2018).

3. Results

3.1. Ambient Stream Chemistry and DOM Properties

The ambient concentrations of DOC, DIN, and PO_4^{3-} at the time of sampling varied widely across the sites and regions (Figure 3). DOC ranged from 0.7 to 27 mg L^{-1} and was higher in smaller streams relative to larger rivers for five of the six regions with longitudinally nested sampling locations (Figure 3a). DOC was negatively correlated with watershed area across sites ($\rho = -0.51$, $n = 22$). The highest DOC concentration occurred at the thermokarst-affected sites in interior Alaska and northwestern Canada (14–27 mg L^{-1}). DIN was uncorrelated with DOC (Figure 3b; $\rho = 0.38$, $n = 22$) and showed a variety of downstream patterns. NO_3^- constituted 65% of DIN on average, but the relative abundance of DIN species (i.e., NO_3^-, NO_2^-, and NH_4^+) varied across sites (supporting information: Background), with NO_3^- ranging from 6.6% at NC1 to 99% of DIN at WA1. NH_4^+ and NO_2^- constituted 26% and 8.8% of DIN on average. PO_4^{3-} was strongly correlated with DOC and to a lesser extent DIN ($\rho = 0.83$ and 0.48, respectively, $n = 19$), with several sites at or near the detection limit (Figure 3). Nutrient concentrations were not correlated with MAT across sites, but DIN and PO_4^{3-} were negatively correlated with MAP ($\rho = -0.49$ and -0.52, $n = 22$ and 19, respectively).

Optical properties of DOM showed as much variability within regions as among them (Figure 4a). There were two initial $SUVA_{254}$ values that exceeded 5 L mg^{-1} m^{-1} (Figure 4a), potentially indicating iron, pH, or NO_3^- interference (Weishaar et al., 2003). There were general decreases in CDOM and HIX moving downstream within regions (Figure 4a), and both parameters were correlated negatively with watershed area across sites ($\rho = -0.46$ and -0.71, respectively, $n = 18$). BIX and TC increased moving downstream for most regions and were positively correlated with watershed area across sites ($\rho = 0.47$ and 0.72, respectively, $n = 18$). FI and $SUVA_{254}$ showed mixed patterns across sites (Figure 4a). CDOM and BIX were corre-

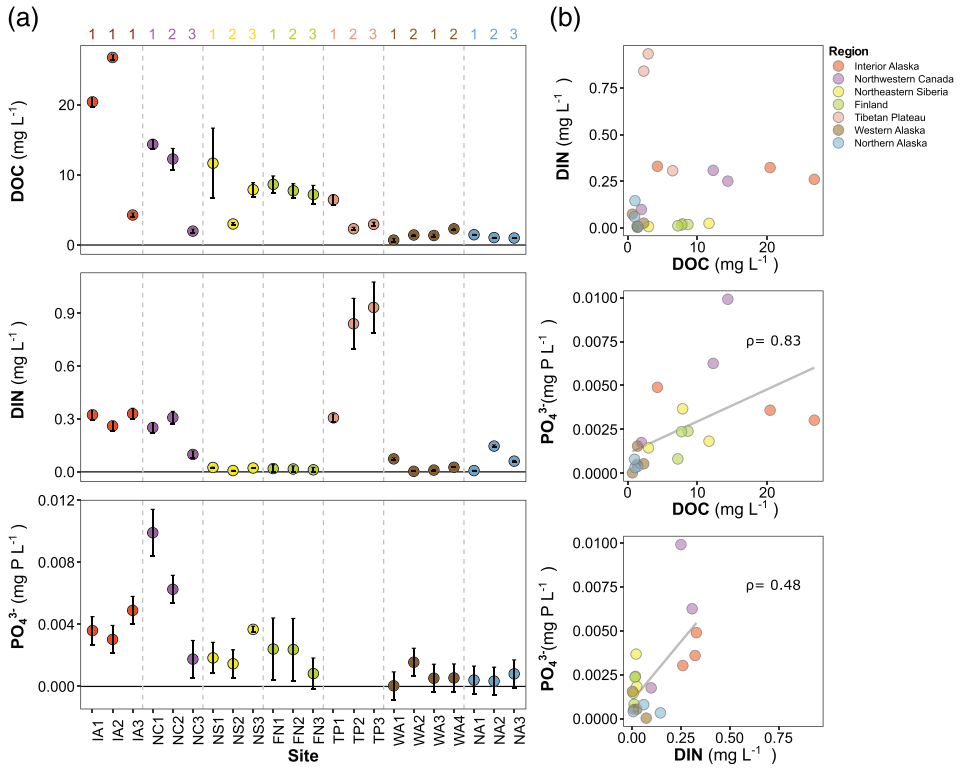

Figure 3. Background nutrient concentrations by site and region. (a) The mean (± standard deviation of three replicates) of dissolved organic carbon (DOC), dissolved inorganic nitrogen (DIN), and phosphate (PO_4^{3-}) in streams from the seven study regions. Regions are separated by the vertical dashed lines and are ordered from highest to lowest mean DOC (left to right). Within regions, sites are ordered by increasing watershed size (longitudinal stream position indicated by the numbering system above the panels) within nested networks, except for IA, where the sites were independent, and WA, where there are two networks. (b) Biplots of mean background nutrient concentrations with Spearman correlation coefficients (ρ) shown when significant ($p < 0.05$). Phosphate was not determined for TP sites because of sample loss during shipping.

lated with MAP ($\rho = -0.62$ and 0.58, respectively, $n = 18$), and $SUVA_{254}$ was negatively correlated with MAT ($\rho = -0.48$, $n = 18$).

There were numerous positive and negative correlations among DOM optical properties and molecular composition (Figure S1), with particularly strong relationships ($|\rho| > 0.65$) between polyphenolics and CDOM ($\rho = 0.79$, $n = 30$), polyphenolics and BIX ($\rho = -0.75$, $n = 30$), unsaturated phenolics (low O/C) and CDOM ($\rho = -0.68$, $n = 30$), and aliphatics and HIX ($\rho = -0.66$, $n = 30$). Molecular composition and to a lesser extent optical properties were also correlated with background nutrient concentrations (Figure S1). DOC and PO_4^{3-} had particularly strong relationships with many parameters, though DIN was also correlated with most molecular composition parameters (Figure S1).

DOM molecular composition was surprisingly similar across regions and sites (Figure 5), in contrast with the high inter- and intra-regional variability in concentrations and bulk optical properties described previously. Despite differences in climate, watershed area, and vegetation, there was strong compositional consistency across sites (Figure 5a). The most abundant compound class was unsaturated phenolics (low O/C), which ranged from 58% to 75% across sites. Unsaturated phenolics (high O/C) were the second most abundant compound class for all but one site in western Alaska (WA1), ranging from 8.5% to 32%. Aliphatics made up less than 9% of the relative abundance for all but one site (also WA1). Polyphenolics and other compounds made up less than 10% of the relative abundance across sites (Figure 5a). DOM molecular compounds were not generally correlated with climate variables, except that polyphenolics were negatively correlated with MAT and MAP ($\rho = -0.70$ and -0.88, $n = 11$), and unsaturated phenolics were correlated with MAP ($\rho = 0.67$ and -0.67 for low and high O/C, respectively, $n = 11$).

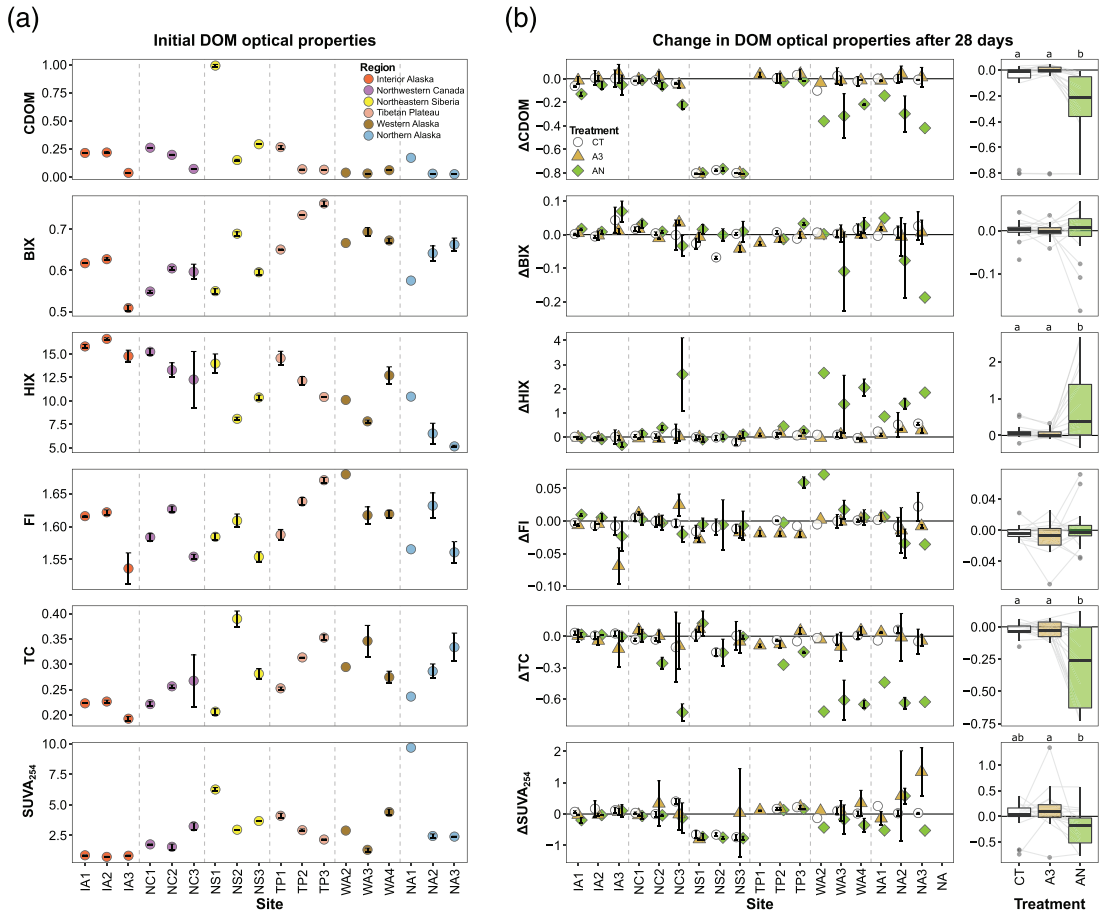

Figure 4. Initial optical properties of dissolved organic matter (DOM) and change through time during the incubations. (a) Initial colored DOM (CDOM), biological index (BIX), humification index (HIX), fluorescence index (FI), peak T to peak C index (TC), and specific UV absorbance at 254 nm ($SUVA_{254}$). (b) Proportional change during the incubation for the three treatments where optical proxies were measured: control (CT), high acetate (A3), and acetate plus nutrients (AN). colored dissolved organic matter (CDOM), biological (mean $n = 3$). for the three treatments where optical measurements were made. In panels (a) and (b), symbology follows Figure 3. Boxplots show the quartiles, median, minimum, and maximum within 1.5 times the interquartile range (IQR) and outliers beyond 1.5 times the IQR. The faint lines behind the boxplots link sites to aid interpretation.

For the multivariate analysis of molecular composition and optical properties, the first three principal components of the PCA explained 86% of the variation in molecular composition and 87% of the variation in optical properties across regions, treatments, and time steps (Figures 6 and S2). The probability ellipses overlapped for all regions, supporting the univariate results of compositional and optical similarity among regions (i.e., greater intra-region than inter-region variability; Figures 6c and 6d).

3.2. DOC Biodegradability and Effects of Priming and Nutrients

The 7- and 28-day incubations revealed relatively low DOC biodegradability but substantial variation among sites (Figures 7, S3, and S4). In the unamended control treatment, proportional change in DOC ranged from −0.01 to −0.22 after 7 days (median and mean $\Delta DOC_7 = -0.06$ and −0.08) and −0.03 to −0.52 after 28 days (median and mean $\Delta DOC_{28} = -0.9$ and −0.16; Figure 7a). ΔDOC_7 and ΔDOC_{28} were positively correlated ($\rho = 0.54$, $n = 19$). The downstream pattern in ΔDOC for sites in nested stream networks differed by region (Figure 7a), and neither ΔDOC_7 nor ΔDOC_{28} was significantly correlated with watershed area ($\rho = -0.27$ and 0.10, respectively, $n = 19$), MAT ($\rho = 0.05$ and 0.01, $n = 19$), or MAP ($\rho = -0.30$ and −0.03, $n = 19$). In the control treatment, ΔDOC_7 was correlated with numerous DOM optical properties and molecular compounds, particularly aliphatics, unsaturated phenolics (high O/C), and HIX (Figure S1). However, ΔDOC_{28} was only correlated with FI (Figure S1). Similarly, control ΔDOC_7 was correlated with background DOC, DIN, and PO_4^{3-} ($\rho = 0.61$, 0.69, and 0.65, respectively), but ΔDOC_{28} was not (Figure S1).

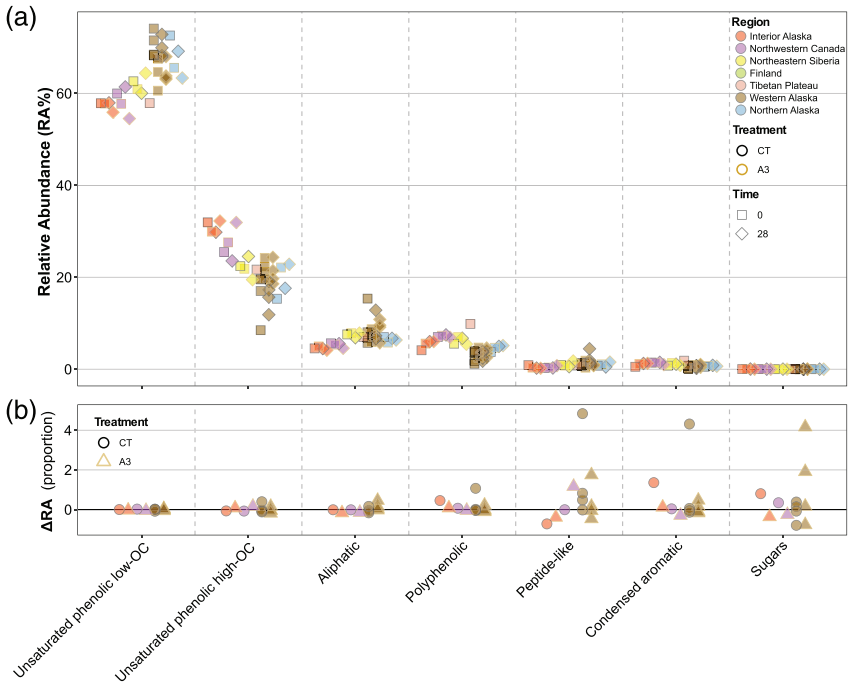

Figure 5. Molecular composition of DOM and change in relative abundance of different components. (a) The relative abundance of composition classes Initial and Final (t_0 and t_{28}). (b) The change in relative abundance expressed as a proportion.

The effects of added acetate and nutrients (i.e., priming and nutrient effects) were not statistically different at 7 and 28 days ($F_{1,239} = 0.15$, $p = 0.69$), so we pooled estimates from both time steps before testing for significance (Figure 7c). We observed negative priming and nutrient effects (i.e., less decrease in DOC) in five of the seven treatments compared to the unamended control (Figure 7c; Bonferroni-corrected p values for each treatment's t test: A1 = 0.0005, A2 = 0.03, A3 = 0.15, N1 = 0.03, N2 = 0.004, N3 = 0.19, and AN = 0.001 0.03, 0.004, and 0.001). Priming and nutrient effects differed by treatment ($F_{1,239} = 3.97$, $p = 0.0009$), with the treatments including acetate showing consistently stronger suppression, reducing median mineralization of background DOM to at or near zero (Figures 7b and 7c). Priming and nutrient effects also differed by site ($F_{1,239} = 4.63$, $p = 1.0 \times 10^{-8}$), with variation in both magnitude and sign of these effects for individual sites (Figures S4 and S5).

The effect of nutrient addition was consistently correlated with ΔDOC across time steps (Figure 8), with neutral or positive nutrient effects at sites with low DOC biodegradability (i.e., ΔDOC ≈ 0) but negative nutrient effects at sites with high DOC biodegradability. The effect of acetate addition was only correlated with ΔDOC for two of the six treatment by time step combinations (Figure 8). The combined effect of nutrient and acetate addition (i.e., the AN treatment) was not correlated with ΔDOC_7 but was correlated with ΔDOC_{28}, with consistently negative effects at sites with biodegradable DOC but neutral to positive effects at sites with lower DOC biodegradability (Figure 8).

3.3. Changes in Acetate, DOM Optical Properties, and DOM Composition

Though we expected complete consumption of added acetate in all treatments, actual ΔAcetate varied in sign and magnitude (Figures 9 and S6). Both the incubation and background data suggested that acetate uptake was nutrient limited. First, acetate uptake was complete in the AN treatment (ΔAcetate range of −0.98 to −1.0), where nutrients were added with acetate (Figure 9). Second, acetate uptake was lower for higher acetate treatments (e.g., the |ΔAcetate| for A3 < A1), suggesting increasing stoichiometric constraints (Figure 9a). Third, there were strong and consistent correlations between background nutrients and ΔAcetate for A1, A2, and A3, with more acetate uptake in sites with higher background nutrient concentrations (Figure 10). ΔAcetate was more strongly correlated with background DOC and PO_4^{3-} than with DIN

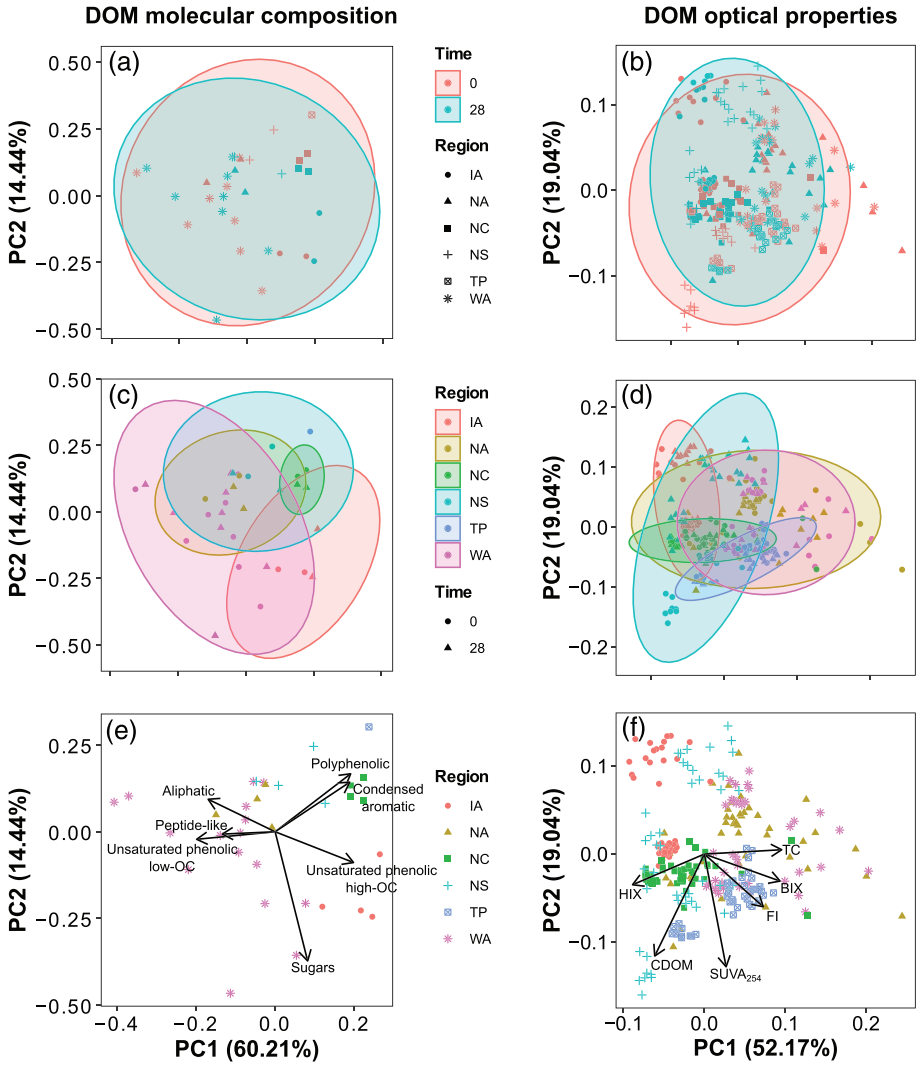

Figure 6. Principal component analysis of the molecular composition and optical properties of DOM. The percentage of variance explained by the first and second principal components (PC1 and PC2) is shown in parentheses next to the axis titles. Parametric probability ellipses are drawn for the indicated groups (i.e., time of sampling in panels a and b and regional provenance of the sample in panels c and d). Loadings for each parameter are shown in panels (e) and (f). PC3 explained 11% of the variation (Figure S2).

(Figure 10). There were no significant correlations between ΔAcetate and nutrient ratios (DOC:DIN, DOC:P-PO_4^{3-}, and DIN:P-PO_4^{3-}) in the acetate amended treatments (Figure S7). For the treatments without acetate addition (i.e., CT, N1, N2, and N3), ΔAcetate was generally negative but highly variable (Figure S6), largely because initial unamended acetate concentration was extremely low across sites (mean ± SD = 0.07 ± 0.1 mg C L^{-1}).

DOM optical properties (which were measured at t_0 and t_{28} for treatments CT, A3, and AN) showed both general and site-specific trends over the course of the experiment (Figures 4 and S8). Across sites, CDOM and TC decreased through time for all three treatments, with significantly larger decreases in the AN treatment (Figure 4b). ΔTC did not show consistent relationships with background chemistry, but ΔCDOM was associated with DIN, with more CDOM loss at sites with lower DIN, lower DIN:P-PO_4^{3-}, and higher DOC:DIN (Figure S9). $SUVA_{254}$ decreased and HIX increased during the experiment, but only for the AN treatment (Figure 4b). ΔHIX was consistently negatively correlated with background DOC and PO_4^{3-}, with greater increases in HIX at lower concentrations (Figure S9). Like for CDOM, Δ$SUVA_{254}$ in the AN treatment was consistently correlated with DIN, with greater decreases in $SUVA_{254}$ at sites with lower t_0 DIN,

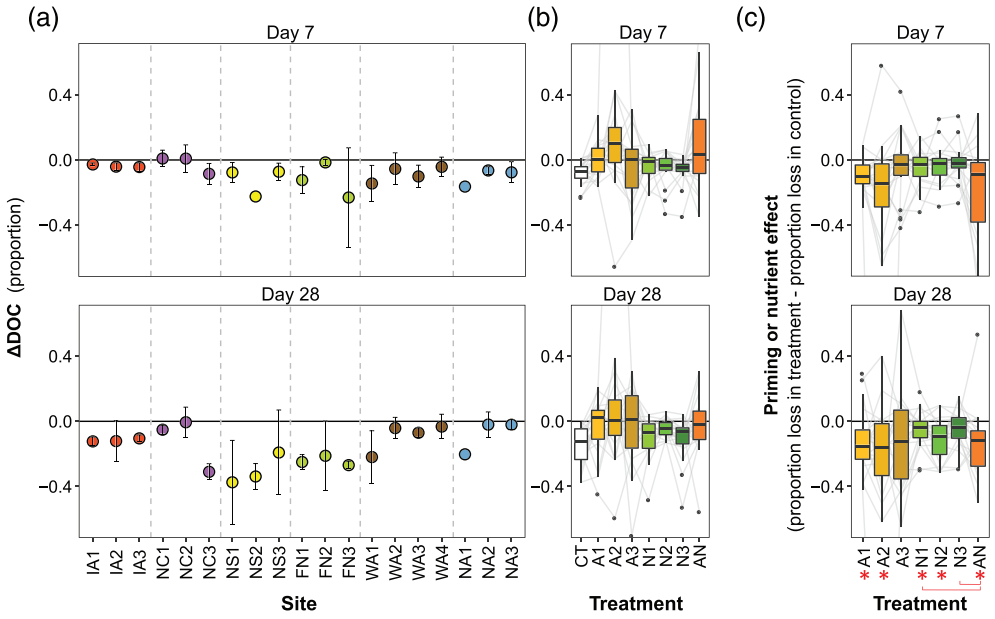

Figure 7. Change in DOC concentration (ΔDOC) after 7 and 28 days and effects of nutrient and acetate addition. (a) Proportional ΔDOC in unamended control treatments by site. (b) Distribution of ΔDOC by treatment. (c) The priming or nutrient effect by treatment expressed as the difference between ΔDOC in the amended treatment and ΔDOC in the unamended control. A positive value represents more DOC loss in the amended treatment (i.e., positive priming or nutrient effect), while a negative value indicates less DOC loss. Asterisks below the *x* axis indicate statistical difference from 0 based on two-sided *t* tests (Bonferroni-adjusted $p < 0.05$), and brackets show statistically significant contrasts among treatments based on Tukey-HSD comparisons following ANOVA (Bonferroni-adjusted $p < 0.05$). Symbology follows Figure 4.

higher DOC:DIN, and lower DIN:P-PO_4^{3-} (Figure S9). Across optical properties, the lower DOC sites (i.e., western and northern Alaska) tended to show greater responses to the AN addition (Figure 4b). The northeastern Siberia sites showed distinct CDOM and $SUVA_{254}$ dynamics, with large decreases in both properties regardless of treatment (Figure 4b).

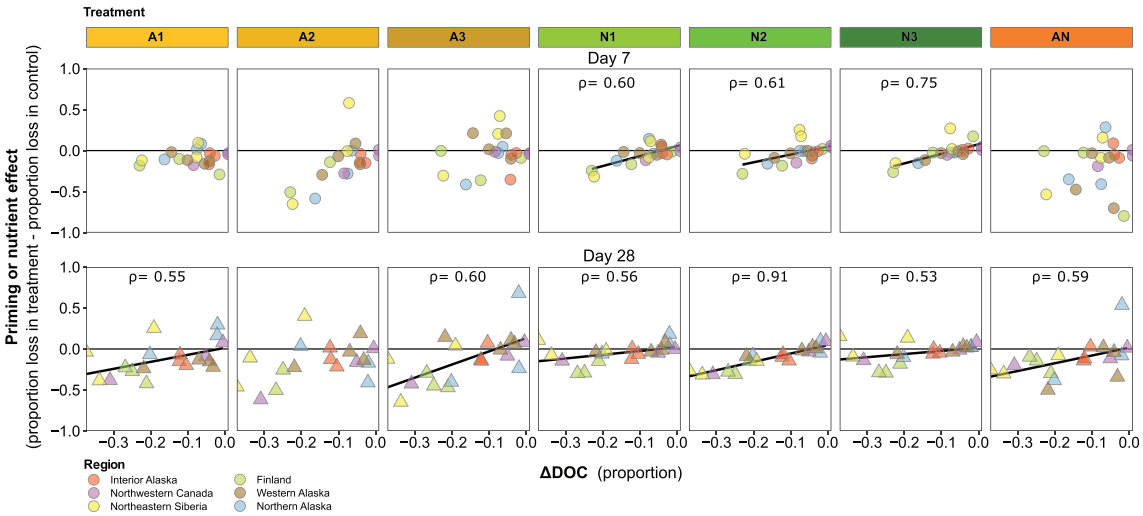

Figure 8. Relationships between ΔDOC in the unamended control treatment and priming or nutrient effects. Positive priming or nutrient effects indicate more DOC loss in the treatment than in the control (i.e., positive priming). Spearman correlation coefficients (ρ) shown when significant ($p < 0.05$). The linear fit lines are shown for convenience, though the Spearman analysis does not assume linearity.

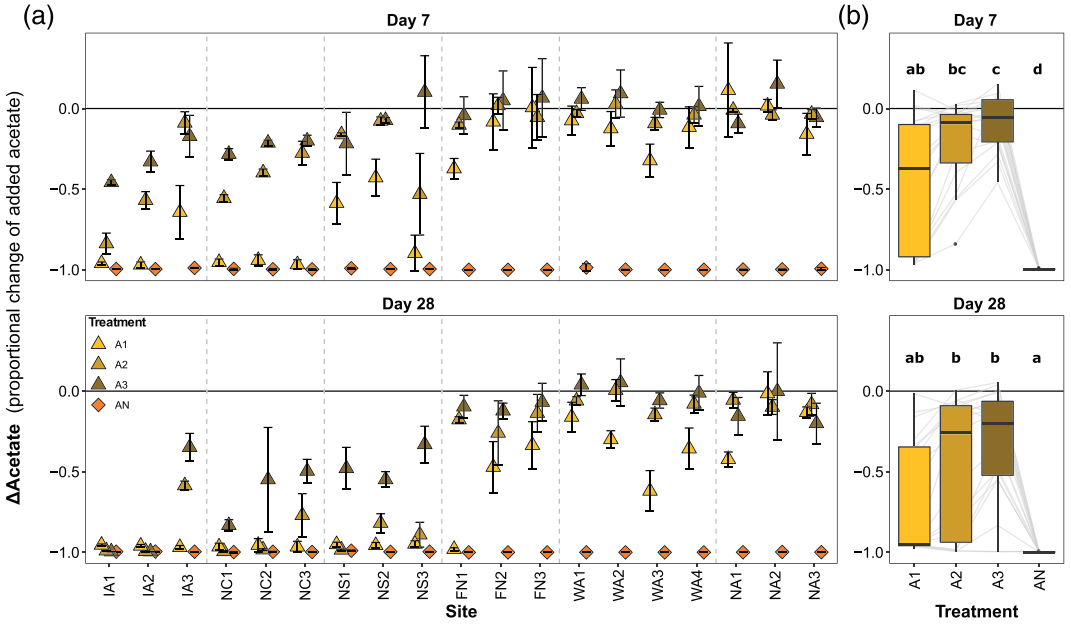

Figure 9. Change in added acetate after 7 and 28 days. (a) Proportional change in added acetate (ΔAcetate) by site. (b) Distribution of ΔAcetate by treatment. Differences in the letters show statistically significant contrasts among treatments based on Tukey-HSD comparisons following ANOVA (Bonferroni-adjusted $p < 0.05$). Symbology follows Figure 4.

DOM molecular composition (which was measured at t_0 and t_{28} for a subset of the CT and A3 treatments) was remarkably stable across the incubations (Figure 5b). The median change in relative abundance was less than 0.05 across all compounds, though there were larger increases or decreases in some of the low-abundance classes, particularly peptide-like compounds and sugars (Figure 5b). However, these changes were largely associated with low initial concentrations and were not consistently associated with treatment (Figure 5b).

The multivariate analysis showed little systematic change in molecular composition and optical properties across treatments (Figures 6a/6b and S2a/S2b). However, individual sites did show substantial shifts, and

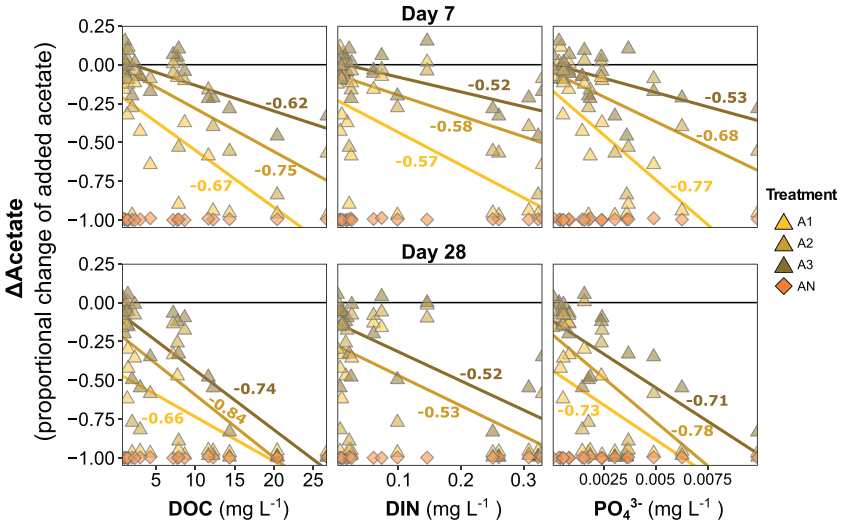

Figure 10. Relationships between change in added acetate and background nutrients. Spearman correlation coefficients (ρ) for each treatment shown when significant ($p < 0.05$). Symbology follows Figure 8.

optical properties showed a slight homogenization (a tighter or smaller probability ellipse) over the course of the experiment (Figures 6b and S2b), in line with the univariate results.

4. Discussion

In this study, we investigated how BDOC and nutrients from thawing permafrost could influence the stability of background DOM in waterways of the permafrost zone. Using optical and molecular characterization techniques in combination with a DOM biodegradability experiment, we found that DOM from across the permafrost zone had surprisingly similar molecular composition, dominated by unsaturated phenolics, but different optical properties and biodegradability. Contrary to our hypotheses, the addition of BDOC and nutrients suppressed the mineralization of background DOM, and there were no systematic differences in DOM biodegradability based on stream network position. These experiments comprise one of the most geographically diverse investigations of aquatic priming to date and our results have several implications for carbon and nutrient balance in the permafrost zone. We discuss the implications and limitations of these findings below.

4.1. DOM Is More Than the Sum of Its Compounds

The similarity in molecular composition of DOM from across permafrost regions supports a growing body of evidence that the building blocks of DOM are similar across freshwater and marine environments (Danczak et al., 2020; Kellerman et al., 2018; Zark & Dittmar, 2018). Because the sources of aquatic DOM vary strongly across ecosystems and through time (e.g., soil, vegetation, and microorganisms), this similarity has mainly been attributed to "filter effects" that select for certain compounds at the dissolution phase and during transport (Gabor, Eilers, et al., 2014; Marín-Spiotta et al., 2014; Roth et al., 2019; Zark & Dittmar, 2018; Zarnetske et al., 2018). A non-exclusive hypothesis for this convergence is that autochthonous production of DOM by aquatic autotrophic and heterotrophic organisms contributes new DOM with a common "aquatic" signature (Harjung et al., 2018; Kellerman et al., 2018; Lee-Cullin et al., 2018). These filtering and aquatic contribution hypotheses have been supported by DOM optical analysis, which shows initial diversity associated with biogeochemical origin followed by convergence toward a more or less universal aquatic DOM signature (Coble et al., 2019; Gabor, Eilers, et al., 2014; Mutschlecner et al., 2018; Wünsch et al., 2019).

This compositional and optical homogeneity of aquatic DOM contrasts with its structural and functional diversity. A wide range of functional experiments and observations have revealed that DOM differs in its interaction with inorganic nutrients, light sensitivity, compound-specific reactivity, and availability to microorganisms in different physico-chemical conditions (Abbott, Jones, et al., 2016; Cory et al., 2014; Dean et al., 2020; Drake et al., 2015; Mu et al., 2017; Nalven et al., 2020; Vonk, Tank, Mann, et al., 2015; Wymore et al., 2015). Even in our relatively limited experiment with filtered, late-summer DOM from cold regions, we observed biodegradability that ranged nearly twentyfold (i.e., 3% to 52%) and priming and nutrient responses that varied in size and sign.

The functional diversity of DOM despite apparent compositional homogeneity implies either that our measures of DOM composition are inadequate (Gabor, Baker, et al., 2014; Hawkes et al., 2020; Simon et al., 2018) or that additional factors regulate DOM persistence and broader ecological function (Figure 11). In either case, this disconnect is problematic because DOM composition is routinely used as a proxy for reactivity, toxicity, and bioavailability (Abbott, Baranov, et al., 2016; Kaiser et al., 2017; Zhang et al., 2019). Additionally, this disconnect suggests that the hope of finding easily measured yet generally applicable proxies of DOM stability—long a goal of aquatic ecosystem science (Balcarczyk et al., 2009; Fellman, Hood, & Spencer, 2010; McDowell et al., 2006)—may continue to be elusive. Both optical and molecular approaches are routinely criticized for ambiguous interpretations, high cost or time investment, and comparability issues among equipment (Benk et al., 2018; Gabor, Baker, et al., 2014; Hawkes et al., 2020; Kellerman et al., 2018; Ruhala & Zarnetske, 2017; Simon et al., 2018). Similarly, empirical measures of DOM function, such as the experiment presented here, have their own suite of limitations. Filtration and isolation of samples from their biotic and abiotic context can demonstrate what is biogeochemically possible rather than what is ecologically relevant (Hanson et al., 2011; James & Boone, 2005; Kothawala et al., 2012). Ultimately DOM characterization, whether optical or molecular, will be most enlightening when coupled with independent measures of DOM function, such as incubations (Cory et al., 2013; Helton et al., 2015; Vonk, Tank, Mann, et al., 2015), in situ processing studies (Ewing et al., 2015; Fork et al., 2020; Hall

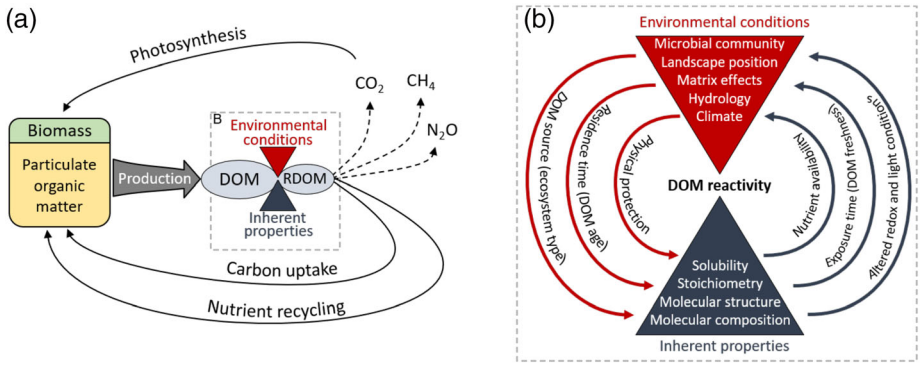

Figure 11. Conceptual model of the carbon cycle emphasizing the role of reactive dissolved organic matter (RDOM) as a choke point or regulator. (a) While biomass and particulate organic matter contain most of the Earth's organic carbon, the pool of reactive DOM as determined by environmental and inherent factors regulates biogeochemical processes such as respiration, nutrient mineralization, methanogenesis, and denitrification. (b) The amount of reactive DOM at a given moment in space and time depends on two-way interactions among environmental conditions and DOM properties. Together, these dynamics regulate the persistence and processing (biotic and abiotic) of DOM. The curved arrows provide examples of links between DOM properties and environmental conditions. The inherent factors that influence DOM degradability are both cause and consequence of the environmental factors that interact to determine realized reactivity (actual rates of DOM alteration, assimilation, or mineralization).

et al., 2016; Harjung et al., 2018; Judd et al., 2006; Mineau et al., 2016), isotope probing experiments (Kellerman et al., 2018; Mulholland, 2004), and characterization of microbial dynamics (Danczak et al., 2020; Guenet et al., 2010; Nalven et al., 2020).

4.2. Intrinsic and Extrinsic Factors Regulate DOM Reactivity Across the Terrestrial-Aquatic Continuum

The perennial debate about intrinsic and extrinsic controls on organic matter stability has extended over decades and across environments from soil to sea (Arnosti, 2004; Ewing et al., 2006; Kellerman et al., 2015; Marín-Spiotta et al., 2014; Schmidt et al., 2011). Until recently, the dominant paradigm was that inherent properties of organic matter determined decay rate, with secondary effects from environmental factors such as temperature, redox, and microbial community (Allison, 2006; Kalbitz et al., 2003; Kleber et al., 2011; Weintraub & Schimel, 2003). Recent observations have challenged this "DOM quality" paradigm, with biodegradable organic matter persisting for centuries in some environments while recalcitrant organic matter is broken down on sub-yearly timescales in others (Arnosti, 2004; Ewing et al., 2006; Kalbitz et al., 2005; Marín-Spiotta et al., 2014; Schmidt et al., 2011). Furthermore, decomposer communities appear to be biochemically omnipotent, breaking down any organic compounds given the right conditions and enough time (Arnosti, 2011; Jaffé et al., 2013; Manzoni et al., 2012; Sinsabaugh et al., 2015). Based on these observations, a new paradigm has been proposed that considers organic matter persistence as an ecosystem property, emphasizing environmental controls such as pH, redox, temperature, light, and physical protection by the soil or water matrix as the determinants of organic matter persistence (Kaiser & Kalbitz, 2012; Lehmann & Kleber, 2015; Marín-Spiotta et al., 2014; Schmidt et al., 2011). According to this ecosystem property hypothesis, the reactivity of organic matter is a function of external factors and has little to do with the initial nutrient content or inherent molecular structure of the organic matter itself.

Both the inherent and ecosystem hypotheses of DOM stability overlook an important internal feedback: DOM concentration and properties are major determinants of many of the environmental conditions that modulate DOM stability in actual ecosystems (Figures 1 and 11). For example, DOM abundance and reactivity influence pH, redox, microbial community, light penetration, nutrient supply, and priming effects (Battin et al., 2008; Fork et al., 2020; Kellerman et al., 2015; Manzoni et al., 2012; Pinay et al., 2015; Zarnetske et al., 2012). These feedbacks (Figure 11) create spatially and temporally dynamic relationships between DOM composition and expressed reactivity (Catalán et al., 2016; Helton et al., 2015; Wymore et al., 2015). Consequently, it is the interaction between inherent DOM composition and ecosystem conditions that determines the relative importance of reaction rates and exposure times for a particular compound

(Abbott, Baranov, et al., 2016; Frei et al., 2020; Kolbe et al., 2019; Oldham et al., 2013). For example, in our dark incubations, the effect of added nutrients or BDOC depended on the decomposability of the background DOM (Figure 8), potentially due to kinetic and nutrient constraints (Guenet et al., 2010; Wymore et al., 2015). However, these responses could vary under different light and nutrient conditions in actual ecosystems, where DOM can act as a nutrient source and light attenuator (Fanta et al., 2010; Fork et al., 2020; Nalven et al., 2020; Rodríguez-Cardona et al., 2016).

These concepts of interactive stability and context-dependent reactivity (Abbott, Baranov, et al., 2016; Kolbe et al., 2019) mean that causal relationships between DOM structure and stability cannot be quantified by correlating DOM characteristics with ecosystem properties such as residence time or climate, though such conclusions are routinely inferred in molecular, optical, and ecosystem studies (Catalán et al., 2016; Cory et al., 2014; Kellerman et al., 2015). This approach does not answer the questions: Did the DOM persist because of its composition and structure, or does it have that structure and composition because it persisted? Similarly, experiments that quantify inherent reactivity isolated from environmental interactions with nutrients and new DOM have limited power to establish causality. We again emphasize that experiments quantifying DOM structure, reactivity, and sensitivity to priming and nutrient effects are needed to establish the relative importance of inherent and ecosystem controls on DOM reactivity in different environments (Danczak et al., 2020; Fork et al., 2020; Guenet et al., 2014; Hotchkiss et al., 2014; Mutschlecner et al., 2017; Nalven et al., 2020; Textor et al., 2019).

4.3. Consequences for Permafrost-Zone Carbon and Nutrient Budgets

The overall negative priming and nutrient effects we observed suggest that permafrost-derived DOC and nutrients are not likely to destabilize modern DOM in high-latitude rivers, lakes, and estuaries. Most high-latitude DOM flux occurs during the snowmelt period, while most permafrost-derived nutrient and DOM release happens in the late thaw season (Abbott et al., 2014; Holmes et al., 2008; Raymond et al., 2007; Spencer et al., 2009; Treat et al., 2016). This means that priming and nutrient effects are unlikely to alter annual net ecosystem carbon balance in permafrost waterways. However, priming and nutrient substrate from degrading permafrost could have important seasonal impacts, depending on background DOM biolability (Figure 8). The few permafrost-zone studies that have quantified seasonal DOM biolability have generally found higher biolability during snowmelt, though some locations experience little seasonal variation, and others have higher biolability in the winter (Abbott et al., 2014; Holmes et al., 2008; Larouche et al., 2015; Mann et al., 2012; Mu et al., 2017; Mutschlecner et al., 2018; Wickland et al., 2012). Permafrost-derived nutrients and BDOC could substantially alter aquatic food webs in the fall and winter by suppressing biolabile DOM processing and stimulating consumption of less biolabile DOM (Figure 8).

While the effects of permafrost-derived material may have seasonally constrained impacts on bulk background DOM, CDOM and other optically defined DOM pools responded strongly to nutrient and BDOC addition (Figure 4). CDOM is a fundamental control on light availability for primary production and penetration of damaging light in high-latitude aquatic and marine ecosystems (Evincent et al., 1998; Fork et al., 2020; Matsuoka et al., 2015; Spencer et al., 2009; Stedmon et al., 2011). If the observed acceleration of CDOM breakdown by nutrients (Figure 4b) is general, the effects could be substantial on aquatic and marine productivity, riverine DOM flux, and microbial communities (Bonilla et al., 2009; Mann et al., 2016; Squires et al., 2002). While long-term nutrient data are sparse for the permafrost zone, there are several indicators that nutrient availability may be increasing in aquatic ecosystems (Abbott et al., 2015; Frey & McClelland, 2009; Kendrick et al., 2018; Shogren et al., 2019). Dynamics including expansion of wildfire, shifts in vegetation, extension of the thaw season, thermokarst formation, and hydrological changes are all increasing the supply and potentially the delivery of nutrients to rivers and lakes in the permafrost zone (Abbott, Jones, et al., 2016; Carey et al., 2019; Hewitt et al., 2018; Rodríguez-Cardona et al., 2020; Salmon et al., 2018; Tank et al., 2020; Treat et al., 2016). We note the need for further research on these CDOM effects because we did not measure change in optical properties in the nutrient only treatments (section 2). This means we cannot isolate whether nutrients alone or the combination of nutrients and BDOC accelerated CDOM breakdown, though the BDOC-only treatment showed no change (Figure 4b).

Finally, the diversity of longitudinal patterns of DOM properties that we observed challenges the simplified view of reactive DOM in the headwaters and stable DOM in larger rivers (Cory et al., 2014; Drake et al., 2015; Mann et al., 2015; Prokushkin et al., 2011; Vonk, Tank, Mann, et al., 2015). While such a longitudinal

decrease in DOM reactivity certainly exists in some watersheds during some parts of the year, broader spatial sampling suggests that headwaters have more diversity in DOM sources and properties compared to larger rivers rather than systematically more reactive DOM (Abbott et al., 2018; Shogren et al., 2019; Zarnetske et al., 2018). More generally, residence time in many permafrost river networks is on the order of days to weeks (Tank et al., 2020), limiting the time biotic and abiotic reactions can modify DOM, even compared with laboratory rates of DOM processing at elevated temperatures (Cory et al., 2013; Vonk, Tank, Mann, et al., 2015). Rather than invoking in-stream processes, changes in DOM sources associated with vegetation, soil and sediment types, and catchment residence times (i.e., water travel time before reaching the channel) can create a variety of longitudinal patterns depending on local ecological context (Abbott et al., 2015; Kling et al., 2000; Tank et al., 2020), including increases, decreases, and convergence toward the watershed mean (Connolly et al., 2018; Neilson et al., 2018; Shogren et al., 2019).

Data Availability Statement

Data and supplementary tables and figures are attached as supplemental information and are available as part of the Hydroshare archive for this work (Abbott & Ewing, 2020), which includes analytical code used to derive figures.

Acknowledgments

E. W. and S. A. E. acknowledge funding from the Montana Agricultural Experimental Station (MAES project number MONB00389) and the National Park Service via the Northwest Alaska and Rocky Mountain Cooperative Ecosystem Study Units (CESUs), as well as the MSU Bayard Taylor Fellowship. B. W. A., J. P. Z., and J. L. C. acknowledge support from the U.S. National Science Foundation (NSF awards: 1446328, 1846855, 1637459, 1916567, and 1916565). J. F. D. and J. E. V. acknowledge funding from the program of the Netherlands Earth System Science Centre (NESSC), financially supported by the Ministry of Education, Culture and Science (OCW; grant number 024.002.001). S. S., S. Z., and S. E. T. acknowledge funding from the Natural Sciences and Engineering Research Council of Canada (NSERC), the Polar Continental Shelf Program, the University of Alberta Northern Research Awards Program, and the Northern Scientific Training Program. M. A. B. recognizes partial NSF support from award numbers 1208732 and 1754216. R. G. M. S and S. R. T. acknowledge funding from NSF (award number 1464392); R. G. M. S., S. R. T., K. P. W., and S. S. W. F. acknowledge funding from the NASA-ABoVE Project 14-14TE-0012 (NNX15AU07A) and the USGS Biological Carbon Sequestration Program; J. O. was supported by funding from the National Park Service Inventory and Monitoring program and the USGS Changing Arctic Ecosystems program. FT-ICR MS performed at the National High Magnetic Field Laboratory ICR User Facility, which is supported by the National Science Foundation Division of Chemistry through DMR-1644779 and the State of Florida. The authors thank all people in the NHMFL ICR Program who work selflessly to facilitate data acquisition and processing for users of the facility. Research reported in this publication was partially supported by Institutional Development Awards (IDeA) from the National Institute of General Medical Sciences of the National Institutes of Health under Awards P20GM103474, U54GM115371, and 5P20GM104417. The content is solely the responsibility of the authors and does not necessarily represent the official views of the National Institutes Health.

References

Aanderud, Z. T., Bahr, J., Robinson, D. M., Belnap, J., Campbell, T. P., Gill, R. A., et al. (2019). The burning of biocrusts facilitates the emergence of a bare soil community of poorly-connected chemoheterotrophic bacteria with depressed ecosystem services. *Frontiers in Ecology and Evolution*, *7*, 467. https://doi.org/10.3389/fevo.2019.00467

Abbott, B. W., Baranov, V., Mendoza-Lera, C., Nikolakopoulou, M., Harjung, A., Kolbe, T., et al. (2016). Using multi-tracer inference to move beyond single-catchment ecohydrology. *Earth Science Reviews*, *160*, 19–42. https://doi.org/10.1016/j.earscirev.2016.06.014

Abbott, B. W., & Ewing, S. (2020). Data and supplementary figures resulting from incubation and analysis of late season stream water from 23 locations within seven northern or high-altitude regions in Asia, Europe, and North America. HydroShare. https://doi.org/10.4211/hs.cb522bbb0f6449ac9d6ca2c189e5c604

Abbott, B. W., Gruau, G., Zarnetske, J. P., Moatar, F., Barbe, L., Thomas, Z., et al. (2018). Unexpected spatial stability of water chemistry in headwater stream networks. *Ecology Letters*, *21*, 296–308. https://doi.org/10.1111/ele.12897

Abbott, B. W., Jones, J. B., Godsey, S. E., Larouche, J. R., & Bowden, W. B. (2015). Patterns and persistence of hydrologic carbon and nutrient export from collapsing upland permafrost. *Biogeosciences*, *12*, 3725–3740. https://doi.org/10.5194/bg-12-3725-2015

Abbott, B. W., Jones, J. B., Schuur, E. A., Chapin, F. S. III, Bowden, W. B., Bret-Harte, M. S., et al. (2016). Biomass offsets little or none of permafrost carbon release from soils, streams, and wildfire: an expert assessment. *Environmental Research Letters*, *11*, 034014. https://doi.org/10.1088/1748-9326/11/3/034014

Abbott, B. W., Larouche, J. R., Jones, J. B., Bowden, W. B., & Balser, A. W. (2014). Elevated dissolved organic carbon biodegradability from thawing and collapsing permafrost. *Journal of Geophysical Research: Biogeosciences*, *119*, 2049–2063. https://doi.org/10.1002/2014JG002678

Allison, S. D. (2006). Brown ground: A soil carbon analogue for the green world hypothesis? *The American Naturalist*, *167*, 619–627. https://doi.org/10.1086/503443

Arnosti, C. (2004). Speed bumps and barricades in the carbon cycle: Substrate structural effects on carbon cycling. *Marine Chemistry*, *92*, 263–273. https://doi.org/10.1016/j.marchem.2004.06.030

Arnosti, C. (2011). Microbial extracellular enzymes and the marine carbon cycle. *Annual Review of Marine Science*, *3*, 401–425. https://doi.org/10.1146/annurev-marine-120709-142731

Baker, A., & Lamont-BIack, J. (2001). Fluorescence of dissolved organic matter as a natural tracer of ground water. *Ground Water*, *39*, 745–750. https://doi.org/10.1111/j.1745-6584.2001.tb02365.x

Baker, M. A., Dahm, C. N., & Valett, H. M. (1999). Acetate retention and metabolism in thehyporheic zone of a mountain stream. *Limnology and Oceanography*, *44*, 1530–1539.

Balcarczyk, K. L., Jones, J. B., Jaffé, R., & Maie, N. (2009). Stream dissolved organic matter bioavailability and composition in watersheds underlain with discontinuous permafrost. *Biogeochemistry*, *94*, 255–270. https://doi.org/10.1007/s10533-009-9324-x

Battin, T. J., Kaplan, L. A., Findlay, S., Hopkinson, C. S., Marti, E., Packman, A. I., et al. (2008). Biophysical controls on organic carbon fluxes in fluvial networks. *Nature Geoscience*, *1*, 95–100. https://doi.org/10.1038/ngeo101

Bengtsson, M. M., Wagner, K., Burns, N. R., Herberg, E. R., Wanek, W., Kaplan, L. A., & Battin, T. J. (2015). No evidence of aquatic priming effects in hyporheic zone microcosms. *Scientific Reports*, *4*(1), 5187. https://doi.org/10.1038/srep05187

Benk, S. A., Li, Y., Roth, V.-N., & Gleixner, G. (2018). Lignin dimers as potential markers for ^{14}C-young terrestrial dissolved organic matter in the critical zone. *Frontiers in Earth Science*, *6*. https://doi.org/10.3389/feart.2018.00168

Bianchi, T. S. (2011). The role of terrestrially derived organic carbon in the coastal ocean: A changing paradigm and the priming effect. *Proceedings of the National Academy of Sciences*, *108*, 19,473–19,481. https://doi.org/10.1073/pnas.1017982108

Bianchi, T. S. (2012). The role of terrestrially derived organic carbon in the coastal ocean: A changing paradigm and the priming effect. *Proceedings of the National Academy of Sciences*, *109*(13), 5134–5134. https://doi.org/10.1073/pnas.1202757109

Bianchi, T. S., Thornton, D. C. O., Yvon-lewis, S. A., King, G. M., Eglinton, T. I., Shields, M. R., et al. (2015). Positive priming of terrestrially derived dissolved organic matter in a freshwater microcosm system. *Geophysical Research Letters*, *42*, 5460–5467. https://doi.org/10.1002/2015GL064765.Received

Bingemann, C. W., Varner, J. E., & Martin, W. P. (1953). The effect of the addition of organic materials on the decomposition of an organic soil. *Soil Science Society of America Proceedings*, *17*, 34–38.

Biskaborn, B. K., Smith, S. L., Noetzli, J., Matthes, H., Vieira, G., Streletskiy, D. A., et al. (2019). Permafrost is warming at a global scale. *Nature Communications*, *10*(1), 264. https://doi.org/10.1038/s41467-018-08240-4

Blagodatsky, S. A., & Richter, O. (1998). Microbial growth in soil and nitrogen turnover: A theoretical model considering the activity state of microorganisms. *Soil Biology and Biochemistry*, *30*(13), 1743–1755. https://doi.org/10.1016/S0038-0717(98)00028-5

Bonilla, S., Rautio, M., & Vincent, W. F. (2009). Phytoplankton and phytobenthos pigment strategies: Implications for algal survival in the changing Arctic. *Polar Biology*, *32*(9), 1293–1303. https://doi.org/10.1007/s00300-009-0626-1

Brahney, J., Ballantyne, A. P., Kociolek, P., Spaulding, S., Otu, M., Porwoll, T., & Neff, J. C. (2014). Dust mediated transfer of phosphorus to alpine lake ecosystems of the Wind River Range, Wyoming, USA. *Biogeochemistry*, *120*, 259–278.

Broadbent, F. E. (1947). Nitrogen release and carbon loss from soil organic matter during decomposition of added plant residues. *Soil Science Society of America Journal*, *12*, 246. https://doi.org/10.2136/sssaj1948.036159950012000C0057x

Brown, J., Ferrians, O., Heginbottom, J. A., & Melnikov, E. (2002). Circum-Arctic Map of Permafrost and Ground-Ice Conditions, Version 2. [Indicate subset used]. Boulder, CO, USA. NSIDC: National Snow and Ice Data Center. https://doi.org/10.7265/skbg-kf16. [April 2020]

Carey, J. C., Abbott, B. W., & Rocha, A. V. (2019). Plant uptake offsets silica release from a large Arctic tundra wildfire. *Earth's Future*, *7*, 1044–1057. https://doi.org/10.1029/2019EF001149

Catalán, N., Kellerman, A. M., Peter, H., Carmona, F., & Tranvik, L. J. (2015). Absence of a priming effect on dissolved organic carbon degradation in lake water. *Limnology and Oceanography*, *60*, 159–168. https://doi.org/10.1002/lno.10016

Catalán, N., Marcé, R., Kothawala, D. N., & Tranvik, L. J. (2016). Organic carbon decomposition rates controlled by water retention time across inland waters. *Nature Geoscience*, *9*, 501–504. https://doi.org/10.1038/ngeo2720

Chen, L., Liu, L., Mao, C., Qin, S., Wang, J., Liu, F., et al. (2018). Nitrogen availability regulates topsoil carbon dynamics after permafrost thaw by altering microbial metabolic efficiency. *Nature Communications*, *9*(1), 3951. https://doi.org/10.1038/s41467-018-06232-y

Chen, L., Liu, L., Qin, S., Yang, G., Fang, K., Zhu, B., et al. (2019). Regulation of priming effect by soil organic matter stability over a broad geographic scale. *Nature Communications*, *10*(1), 5112. https://doi.org/10.1038/s41467-019-13119-z

Coble, A. A., Koenig, L. E., Potter, J. D., Parham, L. M., & McDowell, W. H. (2019). Homogenization of dissolved organic matter within a river network occurs in the smallest headwaters. *Biogeochemistry*, *143*(1), 85–104. https://doi.org/10.1007/s10533-019-00551-y

Coch, C., Ramage, J. L., Lamoureux, S. F., Meyer, H., Knoblauch, C., & Lantuit, H. (2020). Spatial variability of dissolved organic carbon, solutes, and suspended sediment in disturbed low Arctic coastal watersheds. *Journal of Geophysical Research: Biogeosciences*, *125*, e2019JG005505. https://doi.org/10.1029/2019JG005505

Connolly, C., Khosh, M. S., Burkart, G. A., Douglas, T. A., Holmes, R. M., Jacobson, A. D., et al. (2018). Watershed slope as a predictor of fluvial dissolved organic matter and nitrate concentrations across geographical space and catchment size in the Arctic. *Environmental Research Letters*, *13*(10), 104015. https://doi.org/10.1088/1748-9326/aae35d

Corilo, Y. E., Podgorski, D. C., McKenna, A. M., Lemkau, K. L., Reddy, C. M., Marshall, A. G., & Rodgers, R. P. (2013). Oil spill source identification by principal component analysis of electrospray ionization Fourier transform ion cyclotron resonance mass spectra. *Analytical Chemistry*, *85*, 9064–9069. https://doi.org/10.1021/ac401604u

Corilo, Y. E., Rowland, S. M., & Rodgers, R. P. (2016). Calculation of the total sulfur content in crude oils by positive-ion atmospheric pressure photoionization Fourier transform ion cyclotron resonance mass spectrometry. *Energy & Fuels*, *30*, 3962–3966. https://doi.org/10.1021/acs.energyfuels.6b00497

Cory, R. M., Crump, B. C., Dobkowski, J. A., & Kling, G. W. (2013). Surface exposure to sunlight stimulates CO_2 release from permafrost soil carbon in the Arctic. *Proceedings of the National Academy of Sciences*, *110*, 3429–3434.

Cory, R. M., Ward, C. P., Crump, B. C., & Kling, G. W. (2014). Sunlight controls water column processing of carbon in arctic fresh waters. *Science*, *345*, 925–928. https://doi.org/10.1126/science.1253119

Creed, I. F., McKnight, D. M., Pellerin, B. A., Green, M. B., Bergamaschi, B. A., Aiken, G. R., et al. (2015). The river as a chemostat: fresh perspectives on dissolved organic matter flowing down the river continuum R. Smith [ed.]. *Canadian Journal of Fisheries and Aquatic Sciences*, *72*(8), 1272–1285. https://doi.org/10.1139/cjfas-2014-0400

Danczak, R. E., Goldman, A. E., Chu, R. K., Toyoda, J. G., Garayburu-Caruso, V. A., Tolić, N., et al. (2020). Ecological theory applied to environmental metabolomes reveals compositional divergence despite conserved molecular properties. bioRxiv 2020.02.12.946459. doi: https://doi.org/10.1101/2020.02.12.946459

Danger, M., Cornut, J., Chauvet, E., Chavez, P., Elger, A., & Lecerf, A. (2013). Benthic algae stimulate leaf litter decomposition in detritus-based headwater streams: A case of aquatic priming effect? *Ecology*, *94*, 1604–1613. https://doi.org/10.1890/12-0606.1

Dean, J. F., Meisel, O. H., Rosco, M. M., Marchesini, L. B., Garnett, M. H., Lenderink, H., et al. (2020). East Siberian Arctic inland waters emit mostly contemporary carbon. *Nature Communications*, *11*(1), 1627. https://doi.org/10.1038/s41467-020-15511-6

Dean, J. F., van Hal, J. R., Dolman, A. J., Aerts, R., & Weedon, J. T. (2018). Filtration artefacts in bacterial community composition can affect the outcome of dissolved organic matter biolability assays. *Biogeosciences*, *15*(23), 7141–7154. https://doi.org/10.5194/bg-15-7141-2018

de Wit, H. A., Lepistö, A., Marttila, H., Wenng, H., Bechmann, M., Blicher-Mathiesen, G., et al. (2020). Land-use dominates climate controls on nitrogen and phosphorus export from managed and natural Nordic headwater catchments. *Hydrological Processes*, *34*, 4831–4850. https://doi.org/10.1002/hyp.13939

Dittmar, T., Koch, B., Hertkorn, N., & Kattner, G. (2008). A simple and efficient method for the solid-phase extraction of dissolved organic matter (SPE-DOM) from seawater. *Limnology and Oceanography: Methods*, *6*, 230–235. https://doi.org/10.4319/lom.2008.6.230

Dorado-García, I., Syväranta, J., Devlin, S. P., Medina-Sánchez, J. M., & Jones, R. I. (2015). Experimental assessment of a possible microbial priming effect in a humic boreal lake. *Aquatic Sciences*, *78*, 191–202. https://doi.org/10.1007/s00027-015-0425-4

Drake, T. W., Wickland, K. P., Spencer, R. G. M., McKnight, D. M., & Striegl, R. G. (2015). Ancient low-molecular-weight organic acids in permafrost fuel rapid carbon dioxide production upon thaw. *Proceedings of the National Academy of Sciences*, *112*, 13,946–13,951. https://doi.org/10.1073/pnas.1511705112

Estop-Aragonés, C., Olefeldt, D., Abbott, B. W., Chanton, J. P., Czimczik, C. I., Dean, J. F., et al. (2020). Assessing the potential for mobilization of old soil carbon after permafrost thaw: A synthesis of ^{14}C measurements from the northern permafrost region. *Global Biogeochemical Cycles*, *34*, e2020GB006672. https://doi.org/10.1029/2020GB006672

Evincent, W. E., Laurion, I., & Pienitz, R. (1998). Arctic and Antarctic lakes as optical indicators of global change. *Annals of Glaciology*, *27*, 691–696. https://doi.org/10.3189/1998AoG27-1-691-696

Ewing, S. A., O'Donnell, J. A., Aiken, G. R., Butler, K., Butman, D., Windham-Myers, L., & Kanevskiy, M. Z. (2015). Long-term anoxia and release of ancient, labile carbon upon thaw of Pleistocene permafrost. *Geophysical Research Letters*, *42*, 10,730–10,738. https://doi.org/10.1002/2015GL066296

Ewing, S. A., Sanderman, J., Baisden, W. T., Wang, Y., & Amundson, R. (2006). The role of large scale soil structure in organic carbon turnover rates. *Journal of Geophysical Research*, *111*, G03012. https://doi.org/10.1029/2006JG000174

Fanta, S. E., Hill, W. R., Smith, T. B., & Roberts, B. J. (2010). Applying the light: nutrient hypothesis to stream periphyton. *Freshwater Biology*, *55*(5), 931–940. https://doi.org/10.1111/j.1365-2427.2009.02309.x

Farquharson, L. M., Romanovsky, V. E., Cable, W. L., Walker, D. A., Kokelj, S., & Nicolsky, D. (2019). Climate change drives widespread and rapid thermokarst development in very cold permafrost in the Canadian High Arctic. *Geophysical Research Letters*, *46*, 6681–6689. https://doi.org/10.1029/2019GL082187

Fellman, J. B., Hood, E., & Spencer, R. G. M. (2010). Fluorescence spectroscopy opens new windows into dissolved organic matter dynamics in freshwater ecosystems: A review. *Limnology and Oceanography*, *55*(6), 2452–2462. https://doi.org/10.4319/lo.2010.55.6.2452

Fellman, J. B., Spencer, R. G. M., Hernes, P. J., Edwards, R. T., D'Amore, D. V., & Hood, E. (2010). The impact of glacier runoff on the biodegradability and biochemical composition of terrigenous dissolved organic matter in near-shore marine ecosystems. *Marine Chemistry*, *121*, 112–122. https://doi.org/10.1016/j.marchem.2010.03.009

Fork, M. L., Karlsson, J., & Sponseller, R. A. (2020). Dissolved organic matter regulates nutrient limitation and growth of benthic algae in northern lakes through interacting effects on nutrient and light availability. *Limnology and Oceanography Letters*, *5*(6), 417–424. https://doi.org/10.1002/lol2.10166

Frei, R. J., Abbott, B. W., Dupas, R., Gu, S., Gruau, G., Thomas, Z., et al. (2020). Predicting nutrient incontinence in the Anthropocene at watershed scales. *Frontiers in Environmental Science*, *7*. https://doi.org/10.3389/fenvs.2019.00200

Frey, K. E., & McClelland, J. W. (2009). Impacts of permafrost degradation on arctic river biogeochemistry. *Hydrological Processes*, *23*, 169–182. https://doi.org/10.1002/hyp.7196

Gabor, R. S., Baker, A., McKnight, D. M., & Miller, M. P. (2014). Fluorescence indices and their interpretation. In A. Baker, D. M. Reynolds, J. Lead, P. G. Coble, R. G. M. Spencer (Eds.), *Aquatic organic matter fluorescence* (pp. 303–338). Cambridge: Cambridge University Press.

Gabor, R. S., Burns, M. A., Lee, R. H., Elg, J. B., Kemper, C. J., Barnard, H. R., & McKnight, D. M. (2015). Influence of leaching solution and catchment location on the fluorescence of water-soluble organic matter. *Environmental Science & Technology*, *49*, 4425–4432. https://doi.org/10.1021/es504881t

Gabor, R. S., Eilers, K., McKnight, D. M., Fierer, N., & Anderson, S. P. (2014). From the litter layer to the saprolite: Chemical changes in water-soluble soil organic matter and their correlation to microbial community composition. *Soil Biology and Biochemistry*, *68*, 166–176. https://doi.org/10.1016/j.soilbio.2013.09.029

Guenet, B., Danger, M., Abbadie, L., & Lacroix, G. (2010). Priming effect: Bridging the gap between terrestrial and aquatic ecology. *Ecology*, *91*(10), 2850–2861. https://doi.org/10.1890/09-1968.1

Guenet, B., Danger, M., Harrault, L., Allard, B., Jauset-Alcala, M., Bardoux, G., et al. (2014). Fast mineralization of land-born C in inland waters: First experimental evidences of aquatic priming effect. *Hydrobiologia*, *721*, 35–44. https://doi.org/10.1007/s10750-013-1635-1

Guo, D., Wang, H., & Li, D. (2012). A projection of permafrost degradation on the Tibetan Plateau during the 21st century. *Journal of Geophysical Research*, *117*, D05106. https://doi.org/10.1029/2011JD016545

Hall, R. O., Tank, J. L., Baker, M. A., Rosi-Marshall, E. J., & Hotchkiss, E. R. (2016). Metabolism, gas exchange, and carbon spiraling in rivers. *Ecosystems*, *19*(1), 73–86. https://doi.org/10.1007/s10021-015-9918-1

Hamilton, T. D. (2003). Surficial geology of the Dalton Highway (Itkillik-Sagavanirktok rivers) area, southern Arctic foothills, Alaska. PR 121. PR 121 Alaska Division of Geological & Geophysical Surveys.

Hanson, P. C., Hamilton, D. P., Stanley, E. H., Preston, N., Langman, O. C., & Kara, E. L. (2011). Fate of allochthonous dissolved organic carbon in lakes: A quantitative approach. *PLoS ONE*, *6*(7), e21884. https://doi.org/10.1371/journal.pone.0021884

Harjung, A., Sabater, F., & Butturini, A. (2018). Hydrological connectivity drives dissolved organic matter processing in an intermittent stream. *Limnologica*, *68*, 71–81. https://doi.org/10.1016/j.limno.2017.02.007

Hawkes, J. A., D'Andrilli, J., Agar, J. N., Barrow, M. P., Berg, S. M., Catalán, N., et al. (2020). An international laboratory comparison of dissolved organic matter composition by high resolution mass spectrometry: Are we getting the same answer? *Limnology and Oceanography: Methods*, *18*(6), 235–258. https://doi.org/10.1002/lom3.10364

Helton, A. M., Wright, M. S., Bernhardt, E. S., Poole, G. C., Cory, R. M., & Stanford, J. A. (2015). Dissolved organic carbon lability increases with water residence time in the alluvial aquifer of a river floodplain ecosystem. *Journal of Geophysical Research: Biogeosciences*, *120*, 693–706. https://doi.org/10.1002/2014JG002832

Hemingway, J. D. (2018). Ft-Icr Ms Data Analysis Package, Zenodo. Retrieved from https://zenodo.org/record/1158757#.X9Z_1ulKjUI

Hendrickson, C. L., Quinn, J. P., Kaiser, N. K., Smith, D. F., Blakney, G. T., Chen, T., et al. (2015). 21 tesla Fourier transform ion cyclotron resonance mass spectrometer: A national resource for ultrahigh resolution mass analysis. *Journal of the American Society for Mass Spectrometry*, *26*, 1626–1632. https://doi.org/10.1007/s13361-015-1182-2

Hewitt, R. E., Taylor, D. L., Genet, H., McGuire, A. D., & Mack, M. C. (2018). Below-ground plant traits influence tundra plant acquisition of newly thawed permafrost nitrogen. *Journal of Ecology*, *107*(2), 950–962. https://doi.org/10.1111/1365-2745.13062

Holmes, R. M., McClelland, J. W., Peterson, B. J., Tank, S. E., Bulygina, E., Eglinton, T. I., et al. (2012). Seasonal and annual fluxes of nutrients and organic matter from large rivers to the Arctic ocean and surrounding seas. *Estuaries and Coasts*, *35*(2), 369–382. https://doi.org/10.1007/s12237-011-9386-6

Holmes, R. M., McClelland, J. W., Raymond, P. A., Frazer, B. B., Peterson, B. J., & Stieglitz, M. (2008). Lability of DOC transported by Alaskan rivers to the Arctic Ocean. *Geophysical Research Letters*, *35*, L03402. https://doi.org/10.1029/2007GL032837

Horikoshi, M., Tang, Y., Dickey, A., Grenié, M., Thompson, R., Selzer, L., et al. (2020). Data Visualization Tools for Statistical Analysis Results (version 0.4.10), 2020. Retrieved from https://CRAN.R-project.org/package=ggfortify

Hotchkiss, E. R., Hall, R. O., Baker, M. A., Rosi-Marshall, E. J., & Tank, J. L. (2014). Modeling priming effects on microbial consumption of dissolved organic carbon in rivers. *Journal of Geophysical Research: Biogeosciences*, *119*, 982–995.

Iwahana, G., Takano, S., Petrov, R. E., Tei, S., Shingubara, R., Maximov, T. C., et al. (2014). Geocryological characteristics of the upper permafrost in a tundra-forest transition of the Indigirka River Valley, Russia. *Polar Science*, *8*(2), 96–113. https://doi.org/10.1016/j.polar.2014.01.005

Jafarov, E. E., Coon, E. T., Harp, D. R., Wilson, C. J., Painter, S. L., Atchley, A. L., & Romanovsky, V. E. (2018). Modeling the role of preferential snow accumulation in through talik development and hillslope groundwater flow in a transitional permafrost landscape. *Environmental Research Letters*, *13*, 105006. https://doi.org/10.1088/1748-9326/aadd30

Jaffé, R., Ding, Y., Niggemann, J., Vähätalo, A. V., Stubbins, A., Spencer, R. G. M., et al. (2013). Global charcoal mobilization from soils via dissolution and riverine transport to the oceans. *Science*, *340*, 345–347. https://doi.org/10.1126/science.1231476

James, S., & Boone, M. (2005). Aquatic and terrestrial mesocosms in amphibian ecotoxicology. *Applied Herpetology*, *2*(3), 231–257. https://doi.org/10.1163/1570754054507442

Jenkinson, D. S., Fox, R. H., & Rayner, J. H. (1985). Interactions between fertilizer nitrogen and soil nitrogen-the so-called 'priming' effect. *Soil Science*, *36*, 425–444.

Jorgenson, T. M., Frost, G. V., & Dissing, D. (2018). Drivers of landscape changes in coastal ecosystems on the Yukon-Kuskokwim Delta, Alaska. *Remote Sensing*, *10*, 1–27. https://doi.org/10.3390/rs10081280

Judd, K. E., Crump, B. C., & Kling, G. W. (2006). Variation in dissolved organic matter controls bacterial production and community composition. *Ecology*, *87*, 2068–2079. https://doi.org/10.1890/0012-9658(2006)87[2068:VIDOMC]2.0.CO;2

Kaiser, K., Canedo-Oropeza, M., McMahon, R., & Amon, R. M. W. (2017). Origins and transformations of dissolved organic matter in large Arctic rivers. *Scientific Reports*, *7*, 13064. https://doi.org/10.1038/s41598-017-12729-1

Kaiser, K., & Kalbitz, K. (2012). Cycling downwards—Dissolved organic matter in soils. *Soil Biology and Biochemistry*, *52*, 29–32. https://doi.org/10.1016/j.soilbio.2012.04.002

Kalbitz, K., Schmerwitz, J., Schwesig, D., & Matzner, E. (2003). Biodegradation of soil-derived dissolved organic matter as related to its properties. *Geoderma*, *113*, 273–291.

Kalbitz, K., Schwesig, D., Rethemeyer, J., & Matzner, E. (2005). Stabilization of dissolved organic matter by sorption to the mineral soil. *Soil Biology and Biochemistry*, *37*, 1319–1331.

Kellerman, A. M., Guillemette, F., Podgorski, D. C., Aiken, G. R., Butler, K. D., & Spencer, R. G. M. (2018). Unifying concepts linking dissolved organic matter composition to persistence in aquatic ecosystems. *Environmental Science & Technology*, *52*(5), 2538–2548. https://doi.org/10.1021/acs.est.7b05513

Kellerman, A. M., Kothawala, D. N., Dittmar, T., & Tranvik, L. J. (2015). Persistence of dissolved organic matter in lakes related to its molecular characteristics. *Nature Geoscience*, *8*, 454–457. https://doi.org/10.1038/ngeo2440

Kendrick, M. R., Huryn, A. D., Bowden, W. B., Deegan, L. A., Findlay, R. H., Hershey, A. E., et al. (2018). Linking permafrost thaw to shifting biogeochemistry and food web resources in an arctic river. *Global Change Biology*, *24*, 5738–5750. https://doi.org/10.1111/gcb.14448

Keuper, F., Dorrepaal, E., van Bodegom, P. M., van Logtestijn, R., Venhuizen, G., van Hal, J., & Aerts, R. (2017). Experimentally increased nutrient availability at the permafrost thaw front selectively enhances biomass production of deep-rooting subarctic peatland species. *Global Change Biology*, *23*, 4257–4266. https://doi.org/10.1111/gcb.13804

Keuper, F., Wild, B., Kummu, M., Beer, C., Blume-Werry, G., Fontaine, S., et al. (2020). Carbon loss from northern circumpolar permafrost soils amplified by rhizosphere priming. *Nature Geoscience*, *13*(8), 560–565. https://doi.org/10.1038/s41561-020-0607-0

Kicklighter, D. W., Hayes, D. J., McClelland, J. W., Peterson, B. J., McGuire, A. D., & Melillo, J. M. (2013). Insights and issues with simulating terrestrial DOC loading of Arctic river networks. *Ecological Applications*, *23*(8), 1817–1836. https://doi.org/10.1890/11-1050.1

Kleber, M., Nico, P. S., Plante, A., Filley, T., Kramer, M., Swanston, C., & Sollins, P. (2011). Old and stable soil organic matter is not necessarily chemically recalcitrant: Implications for modeling concepts and temperature sensitivity. *Global Change Biology*, *17*(2), 1097–1107. https://doi.org/10.1111/j.1365-2486.2010.02278.x

Kling, G. W., Kipphut, G. W., Miller, M. M., & O'Brien, W. J. (2000). Integration of lakes and streams in a landscape perspective: The importance of material processing on spatial patterns and temporal coherence. *Freshwater Biology*, *43*, 477–497. https://doi.org/10.1046/j.1365-2427.2000.00515.x

Koch, B. P., & Dittmar, T. (2016). From mass to structure: An aromaticity index for high-resolution mass data of natural organic matter. *Rapid Communications in Mass Spectrometry*, *30*, 250–250. https://doi.org/10.1002/rcm.7433

Koch, J. C., Ewing, S. A., Striegl, R., & McKnight, D. M. (2013). Rapid runoff via shallow throughflow and deeper preferential flow in a boreal catchment underlain by frozen silt (Alaska, USA). *Hydrogeology Journal*, *21*(1), 93–106. https://doi.org/10.1007/s10040-012-0934-3

Koch, J. C., Kikuchi, C. P., Wickland, K. P., & Schuster, P. (2014). Runoff sources and flow paths in a partially burned, upland boreal catchment underlain by permafrost. *Water Resources Research*, *50*, 8141–8158. https://doi.org/10.1002/2014WR015586

Kokelj, S. V., Tunnicliffe, J. F., & Lacelle, D. (2017). The Peel Plateau of northwestern Canada: An ice-rich hummocky moraine landscape in transition. In O. Slaymaker (Ed.), *Landscapes and landforms of western Canada* (pp. 109–122). New York: Springer International Publishing.

Kolbe, T., de Dreuzy, J. R., Abbott, B. W., Aquilina, L., Babey, T., Green, C. T., et al. (2019). Stratification of reactivity determines nitrate removal in groundwater. *Proceedings of the National Academy of Sciences*, *116*(7), 2494–2499. https://doi.org/10.1073/pnas.1816892116

Kortelainen, P., Larmola, T., Rantakari, M., Juutinen, S., Alm, J., & Martikainen, P. J. (2020). Lakes as nitrous oxide sources in the boreal landscape. *Global Change Biology*, *26*(3), 1432–1445. https://doi.org/10.1111/gcb.14928

Kothawala, D. N., von Wachenfeldt, E., Koehler, B., & Tranvik, L. J. (2012). Selective loss and preservation of lake water dissolved organic matter fluorescence during long-term dark incubations. *Science of the Total Environment*, *433*, 238–246. https://doi.org/10.1016/j.scitotenv.2012.06.029

Kotz, S., & Nadarajah, S. (2004). *Multivariate t-distributions and their applications*. Cambridge: Cambridge University Press. https://doi.org/10.1017/CBO9780511550683

Krickov, I. V., Lim, A. G., Manasypov, R. M., Loiko, S. V., Vorobyev, S. N., Shevchenko, V. P., et al. (2020). Major and trace elements in suspended matter of western Siberian rivers: First assessment across permafrost zones and landscape parameters of watersheds. *Geochimica et Cosmochimica Acta*, *269*, 429–450. https://doi.org/10.1016/j.gca.2019.11.005

Kuzyakov, Y., Friedel, J. K., & Stahr, K. (2000). Review of mechanisms and quantification of priming effects. *Soil Biology and Biochemistry*, *32*, 1485–1498.

Larouche, J. R., Abbott, B. W., Bowden, W. B., & Jones, J. B. (2015). The role of watershed characteristics, permafrost thaw, and wildfire on dissolved organic carbon biodegradability and water chemistry in Arctic headwater streams. *Biogeosciences*, *12*, 4221–4233. https://doi.org/10.5194/bg-12-4221-2015

Laudon, H., Buttle, J., Carey, S. K., McDonnell, J., McGuire, K., Seibert, J., et al. (2012). Cross-regional prediction of long-term trajectory of stream water DOC response to climate change. *Geophysical Research Letters*, *39*, L18404. https://doi.org/10.1029/2012GL053033

Lee-Cullin, J. A., Zarnetske, J. P., Ruhala, S. S., & Plont, S. (2018). Toward measuring biogeochemistry within the stream-groundwater interface at the network scale: An initial assessment of two spatial sampling strategies. *Limnology and Oceanography: Methods*, *16*, 722–733. https://doi.org/10.1002/lom3.10277

Lehmann, J., & Kleber, M. (2015). The contentious nature of soil organic matter. *Nature*, *528*, 60–68. https://doi.org/10.1038/nature16069

Lepistö, A., Kortelainen, P., & Mattsson, T. (2008). Increased organic C and N leaching in a northern boreal river basin in Finland. *Global Biogeochemical Cycles*, *22*, GB3029. https://doi.org/10.1029/2007GB003175

Littlefair, C. A., & Tank, S. E. (2018). Biodegradability of thermokarst carbon in a till-associated, glacial margin landscape: The case of the Peel Plateau, NWT, Canada. *Journal of Geophysical Research: Biogeosciences*, *123*, 3293–3307. https://doi.org/10.1029/2018JG004461

Littlefair, C. A., Tank, S. E., & Kokelj, S. V. (2017). Retrogressive thaw slumps temper dissolved organic carbon delivery to streams of the Peel Plateau, NWT, Canada. *Biogeosciences*, *14*(23), 5487–5505. https://doi.org/10.5194/bg-14-5487-2017

Liu, F., Chen, L., Zhang, B., Wang, G., Qin, S., & Yang, Y. (2018). Ultraviolet radiation rather than inorganic nitrogen increases dissolved organic carbon biodegradability in a typical thermo-erosion gully on the Tibetan Plateau. *Science of the Total Environment*, *627*, 1276–1284. https://doi.org/10.1016/j.scitotenv.2018.01.275

Liu, F., Kou, D., Abbott, B. W., Mao, C., Chen, Y., Chen, L., & Yang, Y. (2019). Disentangling the effects of climate, vegetation, soil and related substrate properties on the biodegradability of permafrost-derived dissolved organic carbon. *Journal of Geophysical Research: Biogeosciences*, *124*(11), 3377–3389. https://doi.org/10.1029/2018JG004944

Liu, P., Corilo, Y. E., & Marshall, A. G. (2016). Polar lipid composition of biodiesel algae candidates *Nannochloropsis oculata* and *Haematococcus pluvialis* from nano liquid chromatography coupled with negative electrospray ionization 14.5 T Fourier transform ion cyclotron resonance mass spectrometry. *Energy & Fuels*, *30*(10), 8270–8276. https://doi.org/10.1021/acs.energyfuels.6b01514

Löhnis, F. (1926). Nitrogen availability of green manures. *Soil Sci.*, *22*, 253–290. https://doi.org/10.1097/00010694-192610000-00001

Luo, J., Niu, F., Lin, Z., Liu, M., & Yin, G. (2019). Recent acceleration of thaw slumping in permafrost terrain of Qinghai-Tibet Plateau: An example from the Beiluhe Region. *Geomorphology*, *341*, 79–85. https://doi.org/10.1016/j.geomorph.2019.05.020

Lynch, L. M., Machmuller, M. B., Cotrufo, M. F., Paul, E. A., & Wallenstein, M. D. (2018). Tracking the fate of fresh carbon in the Arctic tundra: Will shrub expansion alter responses of soil organic matter to warming? Soil Biol. *The Biochemist*, *120*, 134–144. https://doi.org/10.1016/j.soilbio.2018.02.002

Mack, M. C., Schuur, E. A. G., Bret-Harte, M. S., Shaver, G. R., & Chapin, F. S. (2004). Ecosystem carbon storage in arctic tundra reduced by long-term nutrient fertilization. *Nature*, *431*, 440–443. https://doi.org/10.1038/nature02887

Malone, E. T., Abbott, B. W., Klaar, M. J., Kidd, C., Sebilo, M., Milner, A. M., & Pinay, G. (2018). Decline in ecosystem $\delta^{13}C$ and mid-successional nitrogen loss in a two-century postglacial chronosequence. *Ecosystems*, *21*, 1659–1675. https://doi.org/10.1007/s10021-018-0245-1

Mann, P. J., Davydova, A., Zimov, N., Spencer, R. G. M., Davydov, S., Bulygina, E., et al. (2012). Controls on the composition and lability of dissolved organic matter in Siberia's Kolyma River basin. *Journal of Geophysical Research*, *117*, G01028. https://doi.org/10.1029/2011JG001798

Mann, P. J., Eglinton, T. I., McIntyre, C. P., Zimov, N., Davydova, A., Vonk, J. E., et al. (2015). Utilization of ancient permafrost carbon in headwaters of Arctic fluvial networks. *Nature Communications*, *6*, 7856. https://doi.org/10.1038/ncomms8856

Mann, P. J., Spencer, R. G. M., Hernes, P. J., Six, J., Aiken, G. R., Tank, S. E., et al. (2016). Pan-Arctic trends in terrestrial dissolved organic matter from optical measurements. *Frontiers in Earth Science*, *4*. https://doi.org/10.3389/feart.2016.00025

Manzoni, S., Piñeiro, G., Jackson, R. B., Jobbágy, E. G., Kim, J. H., & Porporato, A. (2012). Analytical models of soil and litter decomposition: Solutions for mass loss and time-dependent decay rates. *Soil Biology and Biochemistry*, *50*, 66–76. https://doi.org/10.1016/j.soilbio.2012.02.029

Marín-Spiotta, E., Gruley, K. E., Crawford, J., Atkinson, E. E., Miesel, J. R., Greene, S., et al. (2014). Paradigm shifts in soil organic matter research affect interpretations of aquatic carbon cycling: Transcending disciplinary and ecosystem boundaries. *Biogeochemistry*, *117*(2-3), 279–297. https://doi.org/10.1007/s10533-013-9949-7

Matsuoka, A., Ortega-Retuerta, E., Bricaud, A., Arrigo, K. R., & Babin, M. (2015). Characteristics of colored dissolved organic matter (CDOM) in the Western Arctic Ocean: Relationships with microbial activities. *Deep-Sea Research Part II: Topical Studies in Oceanography*, *118*, 44–52. https://doi.org/10.1016/j.dsr2.2015.02.012

Mattsson, T., Kortelainen, P., & Räike, A. (2005). Export of DOM from boreal catchments: Impacts of land use cover and climate. *Biogeochemistry*, *76*(2), 373–394. https://doi.org/10.1007/s10533-005-6897-x

McClelland, J. W., Townsend-Small, A., Holmes, R. M., Pan, F., Stieglitz, M., Khosh, M., & Peterson, B. J. (2014). River export of nutrients and organic matter from the North Slope of Alaska to the Beaufort Sea. *Water Resources Research*, *50*, 1823–1839. https://doi.org/10.1002/2013WR014722

McDowell, W. H., Zsolnay, A., Aitkenhead-Peterson, J. A., Gregorich, E. G., Jones, D. L., Jödemann, D., et al. (2006). A comparison of methods to determine the biodegradable dissolved organic carbon from different terrestrial sources. Soil Biol. *The Biochemist*, *38*(7), 1933–1942. https://doi.org/10.1016/j.soilbio.2005.12.018

McGuire, A. D., Anderson, L. G., Christensen, T. R., Dallimore, S., Guo, L., Hayes, D. J., et al. (2009). Sensitivity of the carbon cycle in the Arctic to climate change. *Ecological Monographs*, *79*(4), 523–555. https://doi.org/10.1890/08-2025.1

McKnight, D. M., Boyer, E. W., Westerhoff, P. K., Doran, P. T., Kulbe, T., & Andersen, D. T. (2001). Spectrofluorometric characterization of dissolved organic matter for indication of precursor organic material and aromaticity. *Limnology and Oceanography*, *46*, 38–48. https://doi.org/10.4319/lo.2001.46.1.0038

Mineau, M. M., Wollheim, W. M., Buffam, I., Findlay, S. E. G., Hall, R. O. Jr., Hotchkiss, E. R., et al. (2016). Dissolved organic carbon uptake in streams: A review and assessment of reach-scale measurements. *Journal of Geophysical Research: Biogeosciences*, *121*, 2019–2029. https://doi.org/10.1002/2015JG003204

Mu, C., Schuster, P. F., Abbott, B. W., Kang, S., Guo, J., Sun, S., et al. Permafrost degradation enhances the risk of mercury release on Qinghai-Tibetan Plateau. *Science of the Total Environment*, *708*, 135127. https://doi.org/10.1016/j.scitotenv.2019.135127

Mu, C. C., Abbott, B. W., Wu, X. D., Zhao, Q., Wang, H. J., Su, H., et al. (2017). Thaw depth determines dissolved organic carbon concentration and biodegradability on the northern Qinghai-Tibetan Plateau. *Geophysical Research Letters*, *44*, 9389–9399. https://doi.org/10.1002/2017GL075067

Mulholland, P. J. (2004). The importance of in-stream uptake for regulating stream concentrations and outputs of N and P from a forested watershed: Evidence from long-term chemistry records for Walker Branch Watershed. *Biogeochemistry*, *70*, 403–426. https://doi.org/10.1007/s10533-004-0364-y

Mutschlecner, A. E., Guerard, J. J., Jones, J. B., & Harms, T. K. (2017). Phosphorus enhances uptake of dissolved organic matter in boreal streams. *Ecosystems*, *21*(4), 675–688. https://doi.org/10.1007/s10021-017-0177-1

Mutschlecner, A. E., Guerard, J. J., Jones, J. B., & Harms, T. K. (2018). Regional and intra-annual stability of dissolved organic matter composition and biolability in high-latitude Alaskan rivers. *Limnology and Oceanography*, *63*, 1605–1621. https://doi.org/10.1002/lno.10795

Nalven, S. G., Ward, C. P., Payet, J. P., Cory, R. M., Kling, G. W., Sharpton, T. J., et al. (2020). Experimental metatranscriptomics reveals the costs and benefits of dissolved organic matter photo-alteration for freshwater microbes. *Environmental Microbiology*, *22*(8), 3505–3521. https://doi.org/10.1111/1462-2920.15121

Neilson, B. T., Cardenas, M. B., O'Connor, M. T., Rasmussen, M. T., King, T. V., & Kling, G. W. (2018). Groundwater flow and exchange across the land surface explain carbon export patterns in continuous permafrost watersheds. *Geophysical Research Letters*, *45*, 7596–7605. https://doi.org/10.1029/2018GL078140

Neumann, R. B., Blazewicz, S. J., Conaway, C. H., Turetsky, M. R., & Waldrop, M. P. (2016). Modeling CH4 and CO_2 cycling using porewater stable isotopes in a thermokarst bog in Interior Alaska: Results from three conceptual reaction networks. *Biogeochemistry*, *127*(1), 57–87. https://doi.org/10.1007/s10533-015-0168-2

Nicolsky, D. J., Romanovsky, V. E., Panda, S. K., Marchenko, S. S., & Muskett, R. R. (2017). Applicability of the ecosystem type approach to model permafrost dynamics across the Alaska North Slope. *Journal of Geophysical Research: Earth Surface*, *122*, 50–75. https://doi.org/10.1002/2016JF003852

Nitze, I., Grosse, G., Jones, B. M., Romanovsky, V. E., & Boike, J. (2018). Remote sensing quantifies widespread abundance of permafrost region disturbances across the Arctic and Subarctic. *Nature Communications*, *9*, 5423. https://doi.org/10.1038/s41467-018-07663-3

O'Donnell, J. A., Aiken, G. R., Butler, K. D., Guillemette, F., Podgorski, D. C., & Spencer, R. G. M. (2016). DOM composition and transformation in boreal forest soils: The effects of temperature and organic-horizon decomposition state. *Journal of Geophysical Research: Biogeosciences*, *121*, 2727–2744. https://doi.org/10.1002/2016JG003431.Received

O'Donnell, J. A., Aiken, G. R., Swanson, D. K., Panda, S., Butler, K. D., & Baltensperger, A. P. (2016). Dissolved organic matter composition of Arctic rivers: Linking permafrost and parent material to riverine carbon. *Global Biogeochemical Cycles*, *30*, 1811–1826. https://doi.org/10.1002/2016GB005482

Oldham, C. E., Farrow, D. E., & Peiffer, S. (2013). A generalized Damköhler number for classifying material processing in hydrological systems. *Hydrology and Earth System Sciences*, *17*(3), 1133–1148. https://doi.org/10.5194/hess-17-1133-2013

Olefeldt, D., Goswami, S., Grosse, G., Hayes, D., Hugelius, G., Kuhry, P., et al. (2016). Circumpolar distribution and carbon storage of thermokarst landscapes. *Nature Communications*, *7*(1), 13,043. https://doi.org/10.1038/ncomms13043

Pinay, G., Peiffer, S., de Dreuzy, J. R., Krause, S., Hannah, D. M., Fleckenstein, J. H., et al. (2015). Upscaling nitrogen removal capacity from local hotspots to low stream orders' drainage basins. *Ecosystems*, *18*, 1101–1120. https://doi.org/10.1007/s10021-015-9878-5

Prokushkin, A. S., Pokrovsky, O. S., Shirokova, L. S., Korets, M. A., Viers, J., Prokushkin, S. G., et al. (2011). Sources and the flux pattern of dissolved carbon in rivers of the Yenisey basin draining the Central Siberian Plateau. *Environmental Research Letters*, *6*(4), 045212. https://doi.org/10.1088/1748-9326/6/4/045212

Qu, B., Sillanpää, M., Li, C., Kang, S., Stubbins, A., Yan, F., et al. (2017). Aged dissolved organic carbon exported from rivers of the Tibetan Plateau S. Lin [ed.]. *PLoS ONE*, *12*(5), e0178166. https://doi.org/10.1371/journal.pone.0178166

R Core Team (2018). R: A language and environment for statistical computing, R Foundation for Statistical Computing.

Raymond, P. A., McClelland, J. W., Holmes, R. M., Zhulidov, A. V., Mull, K., Peterson, B. J., et al. (2007). Flux and age of dissolved organic carbon exported to the Arctic Ocean: A carbon isotopic study of the five largest arctic rivers. *Global Biogeochemical Cycles*, *21*, GB4011. https://doi.org/10.1029/2007GB002934

Reyes, F. R., & Lougheed, V. L. (2015). Rapid nutrient release from permafrost thaw in Arctic aquatic ecosystems. *Arctic, Antarctic, and Alpine Research*, *47*, 35–48. https://doi.org/10.1657/AAAR0013-099

Robbins, C. J., King, R. S., Yeager, A. D., Walker, C. M., Back, J. A., Doyle, R. D., & Whigham, D. F. (2017). Low-level addition of dissolved organic carbon increases basal ecosystem function in a boreal headwater stream. *Ecosphere*, *8*, e01739. https://doi.org/10.1002/ecs2.1739

Rodríguez-Cardona, B., Wymore, A. S., & McDowell, W. H. (2016). DOC:NO_3^- ratios and NO_3^- uptake in forested headwater streams. *Journal of Geophysical Research: Biogeosciences*, *121*, 205–217. https://doi.org/10.1002/2015JG003146

Rodríguez-Cardona, B. M., Coble, A. A., Wymore, A. S., Kolosov, R., Podgorski, D. C., Zito, P., et al. (2020). Wildfires lead to decreased carbon and increased nitrogen concentrations in upland arctic streams. *Scientific Reports*, *10*(1), 8722. https://doi.org/10.1038/s41598-020-65520-0

Romanovsky, V. E., Smith, S. L., & Christiansen, H. H. (2010). Permafrost thermal state in the polar Northern Hemisphere during the international polar year 2007–2009: A synthesis. *Permafrost and Periglacial Processes*, *21*, 106–116. https://doi.org/10.1002/ppp.689

Rosemond, A. D., Benstead, J. P., Bumpers, P. M., Gulis, V., Kominoski, J. S., Manning, D. W. P., et al. (2015). Experimental nutrient additions accelerate terrestrial carbon loss from stream ecosystems. *Science*, *347*(6226), 1142–1145. https://doi.org/10.1126/science.aaa1958

Roth, V.-N., Lange, M., Simon, C., Hertkorn, N., Bucher, S., Goodall, T., et al. (2019). Persistence of dissolved organic matter explained by molecular changes during its passage through soil. *Nature Geoscience*, *12*, 755–761. https://doi.org/10.1038/s41561-019-0417-4

Ruhala, S. S., & Zarnetske, J. P. (2017). Using in-situ optical sensors to study dissolved organic carbon dynamics of streams and watersheds: A review. *Science of the Total Environment*, *575*, 713–723. https://doi.org/10.1016/j.scitotenv.2016.09.113

Salmon, V. G., Schädel, C., Bracho, R., Pegoraro, E., Celis, G., Mauritz, M., et al. (2018). Adding depth to our understanding of nitrogen dynamics in permafrost soils. *Journal of Geophysical Research: Biogeosciences*, *123*, 2497–2512. https://doi.org/10.1029/2018JG004518

Schmidt, M. W. I., Torn, M. S., Abiven, S., Dittmar, T., Guggenberger, G., Janssens, I. A., et al. (2011). Persistence of soil organic matter as an ecosystem property. *Nature*, *478*, 49–56. https://doi.org/10.1038/nature10386

Shiklomanov, N. I., Streletskiy, D. A., Nelson, F. E., Hollister, R. D., Romanovsky, V. E., Tweedie, C. E., et al. (2010). Decadal variations of active-layer thickness in moisture-controlled landscapes, Barrow, Alaska. *Journal of Geophysical Research*, *115*, G00I04. https://doi.org/10.1029/2009JG001248

Shogren, A. J., Zarnetske, J. P., Abbott, B. W., Iannucci, F., Frei, R. J., Griffin, N. A., & Bowden, W. B. (2019). Revealing biogeochemical signatures of Arctic landscapes with river chemistry. *Scientific Reports*, *9*, 1–11. https://doi.org/10.1038/s41598-019-49296-6

Simon, C., Roth, V.-N., Dittmar, T., & Gleixner, G. (2018). Molecular signals of heterogeneous terrestrial environments identified in dissolved organic matter: A comparative analysis of Orbitrap and ion cyclotron resonance mass spectrometers. *Frontiers in Earth Science*, *6*. https://doi.org/10.3389/feart.2018.00138

Sinsabaugh, R. L., Shah, J. J. F., Findlay, S. G., Kuehn, K. A., & Moorhead, D. L. (2015). Scaling microbial biomass, metabolism and resource supply. *Biogeochemistry*, *122*, 175–190. https://doi.org/10.1007/s10533-014-0058-z

Slavik, K., Peterson, B. J., Deegan, L. A., Bowden, W. B., Hershey, A. E., & Hobbie, J. E. (2004). Long-term responses of the Kuparuk River ecosystem to phosphorus fertilization. *Ecology*, *85*, 939–954. https://doi.org/10.1890/02-4039

Smith, D. F., Podgorski, D. C., Rodgers, R. P., Blakney, G. T., & Hendrickson, C. L. (2018). 21 tesla FT-ICR mass spectrometer for ultrahigh-resolution analysis of complex organic mixtures. *Analytical Chemistry*, *90*, 2041–2047. https://doi.org/10.1021/acs.analchem.7b04159

Spencer, R. G. M., Aiken, G. R., Butler, K. D., Dornblaser, M. M., Striegl, R. G., & Hernes, P. J. (2009). Utilizing chromophoric dissolved organic matter measurements to derive export and reactivity of dissolved organic carbon exported to the Arctic Ocean: A case study of the Yukon River, Alaska. *Geophysical Research Letters*, *36*, L06401. https://doi.org/10.1029/2008GL036831

Spencer, R. G. M., Mann, P. J., Dittmar, T., Eglinton, T. I., McIntyre, C., Holmes, R. M., et al. (2015). Detecting the signature of permafrost thaw in Arctic rivers. *Geophysical Research Letters*, *42*, 2830–2835. https://doi.org/10.1002/2015GL063498

Squires, M. M., Lesack, L. F. W., & Huebert, D. (2002). The influence of water transparency on the distribution and abundance of macrophytes among lakes of the Mackenzie Delta, Western Canadian Arctic. *Freshwater Biology*, *47*(11), 2123–2135. https://doi.org/10.1046/j.1365-2427.2002.00959.x

Stedmon, C. A., Amon, R. M. W., Rinehart, A. J., & Walker, S. A. (2011). The supply and characteristics of colored dissolved organic matter (CDOM) in the Arctic Ocean: Pan Arctic trends and differences. *Marine Chemistry*, *124*(1-4), 108–118. https://doi.org/10.1016/j.marchem.2010.12.007

Stubbins, A., Mann, P. J., Powers, L., Bittar, T. B., Dittmar, T., McIntyre, C. P., et al. (2016). Low photolability of yedoma permafrost dissolved organic carbon. *Journal of Geophysical Research: Biogeosciences*, *122*, 200–211. https://doi.org/10.1002/2016JG003688

Tank, S. E., Frey, K. E., Striegl, R. G., Raymond, P. A., Holmes, R. M., McClelland, J. W., & Peterson, B. J. (2012). Landscape-level controls on dissolved carbon flux from diverse catchments of the circumboreal. *Global Biogeochemical Cycles*, *26*, GB0E02. https://doi.org/10.1029/2012GB004299

Tank, S. E., Vonk, J. E., Walvoord, M. A., McClelland, J. W., Laurion, I., & Abbott, B. W. (2020). Landscape matters: Predicting the biogeochemical effects of permafrost thaw on aquatic networks with a state factor approach. *Permafrost and Periglacial Processes*, *31*(3), 358–370. https://doi.org/10.1002/ppp.2057

Tanski, G., Lantuit, H., Ruttor, S., Knoblauch, C., Radosavljevic, B., Strauss, J., et al. (2017). Transformation of terrestrial organic matter along thermokarst-affected permafrost coasts in the Arctic. *Science of the Total Environment*, *581-582*, 434–447. https://doi.org/10.1016/j.scitotenv.2016.12.152

Textor, S. R., Guillemette, F., Zito, P. A., & Spencer, R. G. M. (2018). An assessment of dissolved organic carbon biodegradability and priming in blackwater systems. *Journal of Geophysical Research: Biogeosciences*, *123*, 2998–3015. https://doi.org/10.1029/2018JG004470

Textor, S. R., Wickland, K. P., Podgorski, D. C., Johnston, S. E., & Spencer, R. G. M. (2019). Dissolved organic carbon turnover in permafrost-influenced watersheds of interior Alaska: Molecular insights and the priming effect. *Frontiers in Earth Science*, *7*. https://doi.org/10.3389/feart.2019.00275

Toohey, R. C., Herman-Mercer, N. M., Schuster, P. F., Mutter, E. A., & Koch, J. C. (2016). Multidecadal increases in the Yukon River Basin of chemical fluxes as indicators of changing flowpaths, groundwater, and permafrost. *Geophysical Research Letters*, *43*, 12,120–12,130. https://doi.org/10.1002/2016GL070817

Treat, C. C., Wollheim, W. M., Varner, R. K., & Bowden, W. B. (2016). Longer thaw seasons increase nitrogen availability for leaching during fall in tundra soils. *Environmental Research Letters*, *11*, 064013. https://doi.org/10.1088/1748-9326/11/6/064013

Turetsky, M. R., Abbott, B. W., Jones, M. C., Anthony, K. W., Olefeldt, D., Schuur, E. A., et al. (2020). Carbon release through abrupt permafrost thaw. *Nature Geoscience*, *13*(2), 138–143. https://doi.org/10.1038/s41561-019-0526-0

Vonk, J. E., Mann, P. J., Davydov, S., Davydova, A., Spencer, R. G. M., Schade, J., et al. (2013). High biolability of ancient permafrost carbon upon thaw. *Geophysical Research Letters*, *40*, 2689–2693. https://doi.org/10.1002/grl.50348

Vonk, J. E., Tank, S. E., Bowden, W. B., Laurion, I., Vincent, W. F., Alekseychik, P., et al. (2015). Reviews and syntheses: Effects of permafrost thaw on Arctic aquatic ecosystems. *Biogeosciences*, *12*(23), 7129–7167. https://doi.org/10.5194/bg-12-7129-2015

Vonk, J. E., Tank, S. E., Mann, P. J., Spencer, R. G. M., Treat, C. C., Striegl, R. G., et al. (2015). Biodegradability of dissolved organic carbon in permafrost soils and aquatic systems: A meta-analysis. *Biogeosciences*, *12*, 6915–6930. https://doi.org/10.5194/bg-12-6915-2015

Walker, D. A., Daniëls, F. J. A., Matveyeva, N. V., Šibík, J., Walker, M. D., Breen, A. L., et al. (2018). Circumpolar Arctic vegetation classification. *Phytocoenologia*, *48*(2), 181–201. https://doi.org/10.1127/phyto/2017/0192

Wang, T., Yang, D., Yang, Y., Piao, S., Li, X., Cheng, G., & Fu, B. (2020). Permafrost thawing puts the frozen carbon at risk over the Tibetan Plateau. *Science Advances*, *6*, eaaz3513. https://doi.org/10.1126/sciadv.aaz3513

Weintraub, M. N., & Schimel, J. P. (2003). Interactions between carbon and nitrogen mineralization and soil organic matter chemistry in Arctic tundra soils. *Ecosystems*, *6*(2), 129–143. https://doi.org/10.1007/s10021-002-0124-6

Weishaar, J. L., Aiken, G. R., Bergamaschi, B. A., Fram, M. S., Fujii, R., & Mopper, K. (2003). Evaluation of specific ultraviolet absorbance as an indicator of the chemical composition and reactivity of dissolved organic carbon. *Environmental Science & Technology*, *37*, 4702–4708. https://doi.org/10.1021/es030360x

Wickham, H., Chang, W., Henry, L., Pedersen, T.L., Takahashi, K., Wilke, C. & Woo, K. (2020). ggplot2: Create elegant data visualisations using the grammar of graphics.

Wickland, K. P., Aiken, G. R., Butler, K., Dornblaser, M. M., Spencer, R. G. M., & Striegl, R. G. (2012). Biodegradability of dissolved organic carbon in the Yukon River and its tributaries: Seasonality and importance of inorganic nitrogen. *Global Biogeochemical Cycles*, *26*, GB0E03. https://doi.org/10.1029/2012GB004342

Wickland, K. P., Waldrop, M. P., Aiken, G. R., Koch, J. C., Jorgenson, M. T., & Striegl, R. G. (2018). Dissolved organic carbon and nitrogen release from boreal Holocene permafrost and seasonally frozen soils of Alaska. *Environmental Research Letters*, *13*, 065011. https://doi.org/10.1088/1748-9326/aac4ad

Wild, B., Andersson, A., Bröder, L., Vonk, J., Hugelius, G., McClelland, J. W., et al. (2019). Rivers across the Siberian Arctic unearth the patterns of carbon release from thawing permafrost. *Proceedings of the National Academy of Sciences*, *116*(21), 10,280–10,285. https://doi.org/10.1073/pnas.1811797116

Wünsch, U. J., Bro, R., Stedmon, C. A., Wenig, P., & Murphy, K. R. (2019). Emerging patterns in the global distribution of dissolved organic matter fluorescence. *Analytical Methods*, *11*, 888–893. https://doi.org/10.1039/C8AY02422G

Wymore, A. S., Rodríguez-Cardona, B., & McDowell, W. H. (2015). Direct response of dissolved organic nitrogen to nitrate availability in headwater streams. *Biogeochemistry*, *126*, 1–10. https://doi.org/10.1007/s10533-015-0153-9

Yang, M., Nelson, F. E., Shiklomanov, N. I., Guo, D., & Wan, G. (2010). Permafrost degradation and its environmental effects on the Tibetan Plateau: A review of recent research. *Earth Science Reviews*, *103*, 31–44. https://doi.org/10.1016/j.earscirev.2010.07.002

Zark, M., & Dittmar, T. (2018). Universal molecular structures in natural dissolved organic matter. *Nature Communications*, *9*. https://doi.org/10.1038/s41467-018-05665-9

Zarnetske, J. P., Bouda, M., Abbott, B. W., Saiers, J., & Raymond, P. A. (2018). Generality of hydrologic transport limitation of watershed organic carbon flux across ecoregions of the United States. *Geophysical Research Letters*, *45*, 11,702–11,711. https://doi.org/10.1029/2018GL080005

Zarnetske, J. P., Haggerty, R., Wondzell, S. M., & Baker, M. A. (2011). Labile dissolved organic carbon supply limits hyporheic denitrification. *Journal of Geophysical Research*, *116*, G04036. https://doi.org/10.1029/2011JG001730

Zarnetske, J. P., Haggerty, R., Wondzell, S. M., Bokil, V. A., & González-Pinzón, R. (2012). Coupled transport and reaction kinetics control the nitrate source-sink function of hyporheic zones. *Water Resources Research*, *48*, W11508. https://doi.org/10.1029/2012WR011894

Zhang, B., Shan, C., Hao, Z., Liu, J., Wu, B., & Pan, B. (2019). Transformation of dissolved organic matter during full-scale treatment of integrated chemical wastewater: Molecular composition correlated with spectral indexes and acute toxicity. *Water Research*, *157*, 472–482. https://doi.org/10.1016/j.watres.2019.04.002

Zolkos, S., & Tank, S. E. (2020). Experimental evidence that permafrost thaw history and mineral composition shape abiotic carbon cycling in thermokarst-affected stream networks. *Frontiers in Earth Science*, *8*, 152. https://doi.org/10.3389/feart.2020.00152

Zolkos, S., Tank, S. E., & Kokelj, S. V. (2018). Mineral weathering and the permafrost carbon-climate feedback. *Geophysical Research Letters*, *45*, 9623–9632. https://doi.org/10.1029/2018GL078748